UNIVERSITY OF TWENTE.

BIOS
Lab on a Chip group

BEAD SEPARATION

Impedance spectroscopy and dielectrophoresis

May 21, 2014

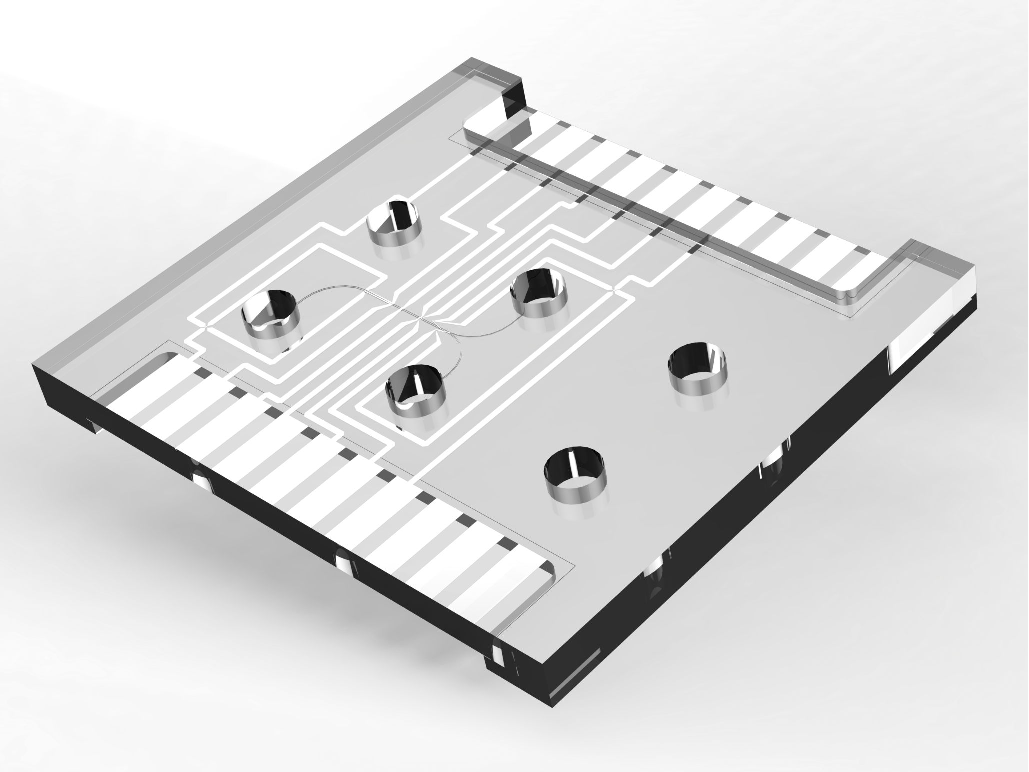

Research chairs:

BIOS

Supervising committee:

Prof.dr.ir. Albert van den Berg
Dr.ir. Wouter Olthuis
Dr.ir. Loes Segerink
Bjorn de Wagenaar, MSc.
Dr.ir. Niels Tas

Faculty:

EEMCS
University of Twente

Student:

Stefan Dekker

Report Number:

2014-4

Summary

The goal of this master project was to create and characterize a microfluidic system that is able to sort polystyrene beads based on their size. These beads had a size of 3 µm or 4 µm, which is in the same order as spermatozoa. Although the scope of the master thesis is limited to working with beads, the system can be used to sort spermatozoa in the future.

The microfluidic system is split up in four parts: differentiation, transport, separation and control. The differentiation of the beads was done with impedance measurements. An equivalent circuit model was developed predicting changes in impedance for a passing bead. Forces produced by dielectrophoresis (DEP) were used to separate the beads. To make the characterization of the different parts easier, several tools were developed. A Labview program on a pc connected to all equipment in the setup made synchronized data acquisition possible. Position data of the beads obtained out of the video could be linked to the impedance data with Matlab scripts.

Characterization of the separate parts showed that the peak height of a peak in the impedance signal can be used to distinguish between 3 µm and 4 µm beads. Focusing with DEP prior to impedance measurements improved the variance in the peak heights corresponding to a single bead size. Furthermore, the width of the peak was used to determine the speed of the bead. Experiments with DEP showed that the trajectory of the bead could be altered. Allowing effective focusing and sorting of beads in the microfluidic channel.

Finally, the control part of the system links all separate function together in a Labview program. Experiments with this system showed that it is able to distinguish between the 3 µm and 4 µm beads using impedance spectroscopy and sort accordingly using dielectrophoresis.

Contents

Chapter 1

Introduction

1.1 Preface

The report in front of you is written as the final part of my master in electrical engineering. The work that I have done during a 32 week period in the BIOS - Lab on a Chip group is described in this report. Before starting my master thesis, I already did a project at the BIOS group which concluded my pre-master. During this project I found out that the interdisciplinary character of the BIOS group fits my interests. So when the time came to do my master thesis I returned.

I want to thank the BIOS - Lab on a Chip group of the EWI department of the University of Twente for the possibility to work on this project, especially Bjorn de Wagenaar for his daily supervision during this project. I also want to thank Loes Segerink and Wouter Olthuis for their input during our meetings. Working at BIOS was pleasant and I want to thank all of you for making this possible.

1.2 The assignment

The goal of the project is to create and characterize a microfluidic system that is able to sort polystyrene beads based on their size. These polystyrene beads have diameters of 3 µm and 4 µm. The functions that the microfluidic system must perform are: differentiate between the different bead sizes, transport the beads, separate the beads and control the link between differentiation and the separation (Fig. 1.1). Existing microfluidic chips fabricated by B. de Wagenaar are used in this project. These microfluidic chips already contain the technology required to implement most of the functions described above. Impedance spectroscopy is used to differentiate between the different bead sizes. The beads are transported by the electrolyte solution flow from the differentiation part to the separation part of the microfluidic chip. The separation is implemented with dielectrophoresis.

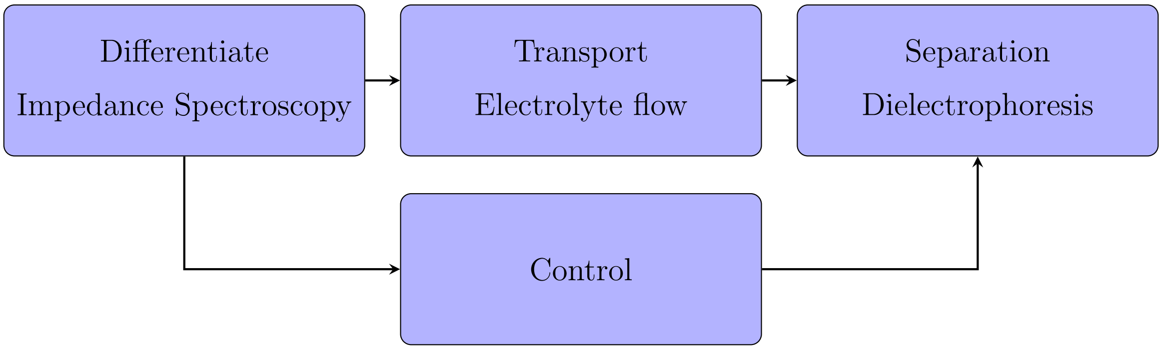

Figure 1.1: Functions of the microfluidic system to be designed.

This research is part of a larger project running in the BIOS group called: "Sex-sorting of spermatozoa on-chip". The goal of this project is to develop a microfluidic device, which is able to sort spermatozoa based on their X- or Y- chromosome content. In the animal industry, it is common to produce offspring using artificial insemination. In nature, the ratio of male/female offspring is 50%. To get a 50% male/female offspring rate, nature made a great effort to make the spermatozoa very similar. Some livestock industries benefit from the offspring of one specific sex e.g. milk cows. For these industries the use of sexed spermatozoa could provide a big financial benefit.

Currently fluorescence-activated cell sorting (FACS) is the only commercial available technique to sex spermatozoa. Although this technique is expensive, it is used in some countries to produce cattle and horses [1]. Sorting is possible due to a difference in the amount of DNA the X- and Y- chromosome are carrying. In a FACS procedure, the DNA in the spermatozoa is labelled with a fluorescent dye called Hoechst 33342. During sorting, the spermatozoa pass a laser with a fluorescence detector one by one. Spermatozoa with an X chromosome will fluoresce brighter, because of the larger DNA content. The signal from the fluorescence detector is used to decide how to charge the droplet carrying the spermatozoa. This charge is used to electrostatically deflect the droplets and thereby sorting the spermatozoa into separate fractions.

As mentioned before, the research presented in this report is part of a larger project. This sub project is focused on the separation of 3 µm and 4 µm beads using an already existing microfluidic chip. Firstly, the functions of the microfluidic setup are optimized individually. Secondly, a control part will be designed to integrate the separate features into a single program, allowing the separation of 3 µm and 4 µm beads. The information obtained in this sub project can be used in the future to separate spermatozoa with the same microfluidic platform.

1.3 Outline

This report starts with the chapter theory and modelling, which focusses on impedance spectroscopy and dielectrophoresis (DEP). The theory behind these techniques is explained and simulations are performed. Subsequently, the materials and methods chapter describes the instrumentation and the developed measurement protocols. The control part of the system is interconnected with the measurement setup and therefore included in the materials and methods section. Experimental results are compared with the simulations and discussed in the results and discussion section. Finally, the project highlights and recommendations are summarized in the conclusions and recommendations section.

Chapter 2

Theory and Modelling

2.1 Impedance Spectroscopy

To differentiate between the different bead sizes in the microfluidic system, impedance spectroscopy is used. Impedance spectroscopy is a technique that uses an applied electrical field to probe a sample. By doing so, information about the dielectrical properties of the sample can be obtained.

In the proposed system, the sample consist of either only the electrolyte solution or a mixture of the electrolyte solution and a polystyrene bead. For both scenario, simulations are constructed to predict the impedance spectrum that is expected. The sample volume is the part of the fluidic channel that is between the electrode on top of the channel and the electrode on the bottom of the channel (Fig. 2.1).

The equivalent circuit model proposed in this chapter uses the Maxwell mixture theory to predict the electrical behaviour of electrolyte and the bead. The double layer capacitance is used to predict the behaviour of the interface between the electrolyte and the electrode.

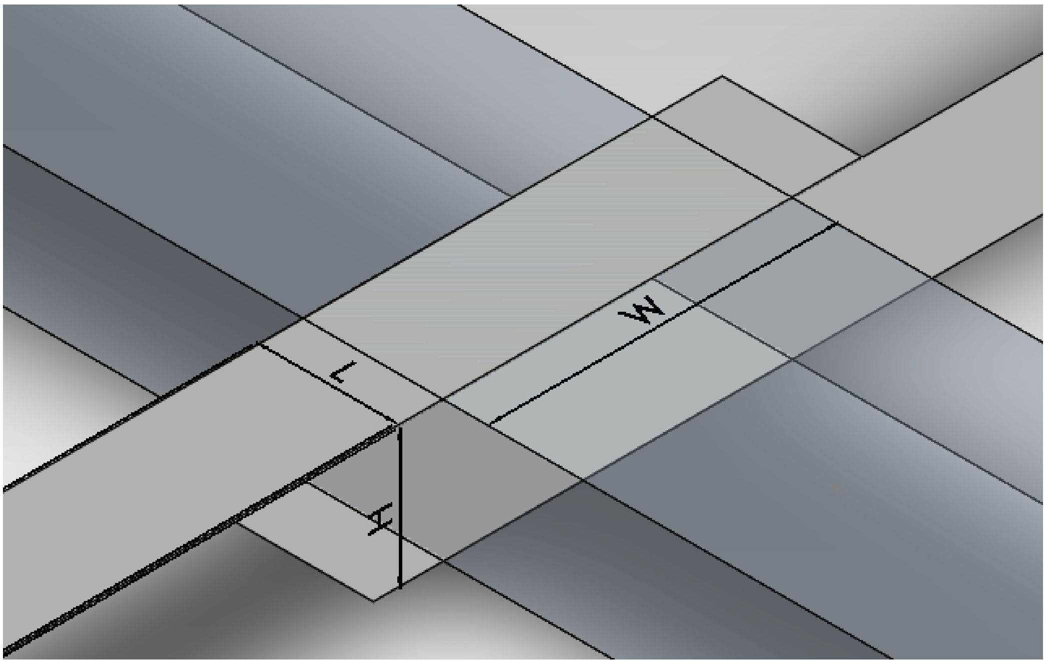

Figure 2.1: Schematic representation of the differentiation part of the microfluidic system. Typical dimensions used in this project are 20 µm for the channel height(H) and the electrode length(L). The width of the channel(W) is 20 or 50 µm.

2.1.1 Maxwell mixture theory

The permittivity of a material is a measure of how easily a material polarizes in response to an electric field. This polarization takes place as bound charges in the material are slightly shifted in their position by an electric field. For the scenario where the sample volume is filled with only electrolyte solution, the permittivity can be found in literature. The scenario where there is a mixture of the electrolyte solution and a polystyrene bead between the electrodes, Maxwell's mixture theory can be used to determine the electrical behaviour of the mixture[2]. The theory translates the dielectrical properties of homogeneous individual components of the mixture into the dielectrical properties of a fictional homogeneous bulk material under the assumption of a homogeneous electric field. According to Maxwell's theory, the permittivity of a mixture of a medium with homogeneous spherical particles can be described by equation 2.1.

$$\tilde{\varepsilon}_{mix} = \tilde{\varepsilon}_m \frac{1 + 2\Phi \tilde{f}_{CM}}{1 - \Phi \tilde{f}_{CM}} \tag{2.1}$$

In equation 2.1 $\tilde{\varepsilon}_{mix}$ and $\tilde{\varepsilon}_m$ represent the permittivity of the mixture and the permittivity of the medium. Φ represents the volume ratio of the particles with respect to the medium. $\tilde{f}_{CM}$ represents the Clausius-Mossoti factor, which is calculated by equation 2.2. The tildes in the equations indicate that the variables are complex. The particle and medium consist of lossy material therefore have conductive properties. This conductance is included in the permittivity as a complex part (eq. 2.3)[3]. In these equations, ε_i and σ_i represent the relative permittivity and conductivity of the particle or the medium.

$$\tilde{f}_{CM} = \frac{\tilde{\varepsilon}_p - \tilde{\varepsilon}_m}{\tilde{\varepsilon}_p + 2\tilde{\varepsilon}_m} \tag{2.2}$$

$$\tilde{\varepsilon}_i = \varepsilon_0 \varepsilon_i - \frac{j\sigma_i}{\omega} \tag{2.3}$$

Imagine an ideal parallel plate electrode configuration with a medium particle suspension between the plates. The impedance of this configuration is given by equation 2.4 [2] where g is the gap between the electrodes and A the area of the electrodes.

$$\tilde{Z}_{mix} = \frac{g}{j\omega\tilde{\varepsilon}_{mix}A} \tag{2.4}$$

$$\tilde{\varepsilon}_{mix} = \frac{1 + 2\Phi \tilde{f}_{CM}}{1 - \Phi \tilde{f}_{CM}} \tag{2.5}$$

$$\tilde{\varepsilon}_{mix} = \frac{1 + 2\Phi \frac{\tilde{\varepsilon}_p - \tilde{\varepsilon}_m}{\tilde{\varepsilon}_p + 2\tilde{\varepsilon}_m}}{1 - \Phi \frac{\tilde{\varepsilon}_p - \tilde{\varepsilon}_m}{\tilde{\varepsilon}_p + 2\tilde{\varepsilon}_m}} \tag{2.6}$$

If $\tilde{\varepsilon}_{mix}$ is substituted in equation 2.4 with equation 2.6, then the equation gets quite long. Therefore, a few derivative steps are not displayed. After multiple manipulations, equation 2.11 is formed [2].

$$\begin{aligned}
\varepsilon_\infty &= \varepsilon_m \frac{2\varepsilon_m + \varepsilon_p - 2\Phi(\varepsilon_m - \varepsilon_p)}{2\varepsilon_m + \varepsilon_p + \Phi(\varepsilon_m - \varepsilon_p)} && (2.7)\\
\sigma_0 &= \sigma_m \frac{2\sigma_m + \sigma_p - 2\Phi(\sigma_m - \sigma_p)}{2\sigma_m + \sigma_p + \Phi(\sigma_m - \sigma_p)} && (2.8)\\
\Delta\varepsilon &= \frac{9(\varepsilon_m\sigma_p - \varepsilon_p\sigma_m)^2\Phi(1-\Phi)}{(2\varepsilon_m + \varepsilon_p + \Phi(\varepsilon_m - \varepsilon_p))(2\sigma_m + \sigma_p + \Phi(\sigma_m - \sigma_p))^2} && (2.9)\\
\tau &= \frac{2\varepsilon_m + \varepsilon_p + \Phi(\varepsilon_m - \varepsilon_p)}{2\sigma_m + \sigma_p + \Phi(\sigma_m - \sigma_p)} && (2.10)\\
\tilde{Z}_{mix} &= \frac{g}{A}\frac{1}{j\omega\varepsilon_\infty + \sigma_o + \frac{j\omega\Delta\varepsilon}{1+j\omega\tau}} && (2.11)
\end{aligned}$$

Equation 2.11 looks like the impedance of a parallel circuit of a capacitor, a resistor and another contribution in parallel. Equation 2.12 describes the impedance of the circuit displayed in figure 2.2. By matching equation 2.11 with 2.12 equations for the network elements can be found. These equations will be in terms of permittivity and conductivity of both the particle and the medium. Hereby an equivalent circuit model is found describing the electrical behaviour of the mixture.

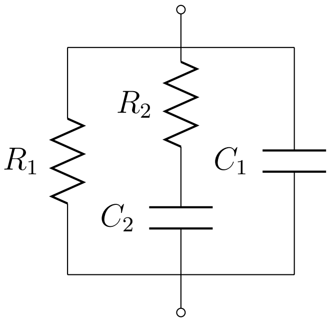

Figure 2.2: Circuit used to fit to the Maxwell mixture theory.

$$\tilde{Z}_{cir} = \frac{1}{j\omega C_1 + \frac{1}{R_1} + \frac{j\omega C_2}{1+j\omega C_2 R_2}} \qquad (2.12)$$

with

$$\begin{aligned}
C_1(\varepsilon_m, \varepsilon_p, \Phi) &= \frac{\varepsilon_\infty A}{g} = \frac{A}{g}\varepsilon_m \frac{2\varepsilon_m + \varepsilon_p - 2\Phi(\varepsilon_m - \varepsilon_p)}{2\varepsilon_m + \varepsilon_p + \Phi(\varepsilon_m - \varepsilon_p)} && (2.13)\\
R_1(\sigma_m, \sigma_p, \Phi) &= \frac{g}{\sigma_0 A} = \frac{g}{A}\frac{2\sigma_m + \sigma_p + \Phi(\sigma_m - \sigma_p)}{\sigma_m(2\sigma_m + \sigma_p - 2\Phi(\sigma_m - \sigma_p))} && (2.14)\\
C_2(\varepsilon_m, \varepsilon_p, \sigma_m, \sigma_p, \Phi) &= \frac{\Delta\varepsilon A}{g} && (2.15)\\
R_2(\varepsilon_m, \varepsilon_p, \sigma_m, \sigma_p, \Phi) &= \frac{\tau}{C_2} && (2.16)
\end{aligned}$$

2.1.2 Electrical double layer

The electric field across the sample volume is applied by setting a certain potential across the top and bottom electrode. No electric field exists inside a metal, which indicates that al charge is at surface of the electrodes. Ions of opposite charge in the electrolyte solution will be attracted to the electrode/electrolyte interface.

Helmholtz was the first to propose a model for this effect[4]. In the Helmholtz model, the charge in the solution is considered as a sheet of ions of the opposite sign compared to the charged surface. Now the interface consist of two sheets of charge, one present at the surface of the electrodes and one of ions in the electrolyte solution. That is were the name double layer originates. The two layers have a separation distance in the order of single molecules. This structure is very similar to a parallel plate capacitor. The capacitance per unit area of such a structure is given by equation 2.17[4].

$$C_H = \frac{\epsilon\epsilon_0}{d} \tag{2.17}$$

$\epsilon\epsilon_0$ is the permittivity of the solute and d the distance between the two layers of charge. Equation 2.17 indicates that the double layer capacitance is constant. From experimental data, it is know that the double layer capacitance varies with applied potential and electrolyte concentration. Therefore, a more advanced model is required.

Gouy and Chapman came up with an alternative model that includes both electrostatic forces and thermal processes[4]. They described the Brownian motion in the solution causing attracted ions to randomly diffuse away from the surface. In the solution a certain volume holds a net charge, balancing the surface charge on the electrode. Near the electrode, the concentration of ions with opposite charge is the largest due to the large electrostatic forces. When moving away from the electrode surface , the electric field is decreasing. As a result, the concentration of anions and cations is becoming more balanced until there is no net charge. The region from the electrode surface to the point where the net charge is zero is called the diffusive layer.

$$C_{G\&C} = (\frac{2z^2e^2\epsilon\epsilon_0 n^0}{kT})^{\frac{1}{2}} \cosh(\frac{ze\phi}{2kT}) \tag{2.18}$$

Equation 2.18[4] gives the double layer capacitance for a symmetric electrolyte according to Gouy-Chapman. ϵ represents the relative permittivity of the electrolyte, ϵ_0 is the vacuum permittivity, z represents the ion charge, e is the elementary charge, n represents bulk ion concentration, k is the Boltzmann constant, T represents the temperature and finally ϕ represents the zeta potential. This model corresponds well with experimental data for low ion concentrations and low potentials. In cases with high potentials or high ion concentrations it predicts too high value for the double layer capacitance. The finite size of ions is not considered and the ions are modelled as point charges. This overestimation is caused by this fact.

Stern made a modification to the Gouy-Chapman theory by combining the Helmholtz stationary layer theory with the diffused layer theory of Gouy-Chapman[4]. Ions with a finite size cannot get infinity close to the electrode surface. Stern proposed to define a plane of closest approach called the outer Helmholtz plane. Between this plane and the electrode, no charge can exist since ions can not get into this region because of their size. From the outer Helmholtz plane into the solution the diffusive layer exist. At high potentials and ion concentrations the charges in the diffusive layer will be tightly packed at the outer Helmholtz plane, behaving in the same way as Helmholtz model would do. At low potentials and low concentrations the charge in the solution is spread over a larger volume, so Sterns modification behaves more like the Gouy-Chapman model.

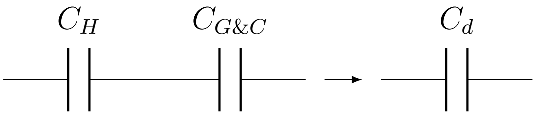

$$\frac{1}{C_d} = \frac{1}{C_H} + \frac{1}{C_{C\&G}} \tag{2.19}$$

Figure 2.3: Sterns modifications and resulting double layer capacitance[4].

$$\frac{1}{C_d} = \frac{x_2}{\epsilon\epsilon_0} + \frac{1}{(\frac{2z^2e^2\epsilon\epsilon_0 n^0}{kT})^{\frac{1}{2}}\cosh(\frac{ze\phi_2}{2kT})} \tag{2.20}$$

Fig. 2.3 shows how the double layer capacitance is formed in the Gouy-Chapman-Stern model[4]. The potential between C_H and $C_{G\&H}$ is the potential at the outer Helmholtz plane. Equation 2.20[4] gives the double layer capacitance in the Gouy-Chapman-Stern model for a symmetric electrolyte. x_2 is the position of outer Helmholtz plane with respect to the electrode, ϕ_2 is the potential at this point.

2.1.3 Equivalent electrical circuit

In this section two equivalent circuits are proposed. One for the scenario where a bead is present in the sample volume and one where there is no bead in the sample volume. First a complete equivalent circuit model is needed. In fig. 2.4 such a circuit is given. The connections to the system are indicated with lines with open rounds at the top and bottom of the figure. The C_{dl} models the electrical double layer as discussed in section 2.1.2. Z_{sample} represents the impedance of the sample volume between the electrodes. This is the circuit element that is influenced by the presence of a bead in the sample volume. C_{par} represents the parasitic capacitance of the system.

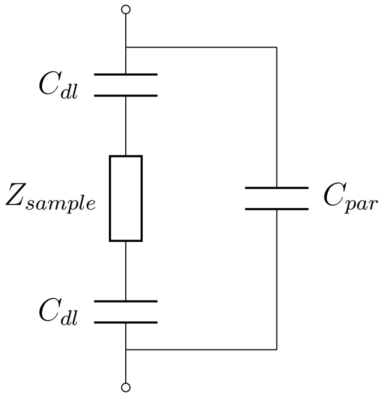

Figure 2.4: Equivalent electrical circuit

Z_{sample} is the most interesting component, as its value will change depending on the sample between the electrodes. Figures 2.5 and 2.6 show the equivalent circuits for both the scenarios. The impedance of the sample volume with a bead is thoroughly discussed in section 2.1.1. In the scenario where only electrolyte is present between the electrodes, the conductivity and permittivity of the electrolyte can be modelled with a simple resistor and capacitor.

In section 2.1.1 equations for all the elements of the circuit in fig. 2.6 are described. Comparing these with the equations for the situation without beads is interesting. Resistor R_1 can be expressed in R_{el} times a factor and C_1 can be expressed in C_{el} times a factor. These factors give the difference in electrical behaviour between the two scenarios. For C_2 and R_2 such simple equation cannot be found.

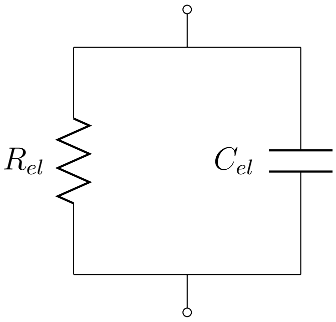

Figure 2.5: Z_{sample} without bead

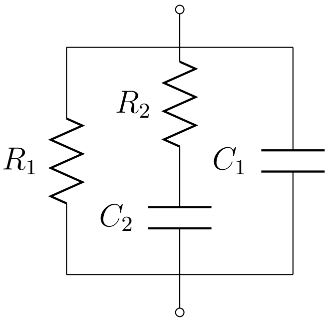

Figure 2.6: Z_{sample} with bead

$$R_{el} = \frac{h}{\sigma_{el} A} \tag{2.21}$$

$$C_{el} = \frac{\varepsilon_0 \varepsilon A}{h} \tag{2.22}$$

$$R_1 = R_{el} \frac{2\sigma_m + \sigma_p + \Phi(\sigma_m - \sigma_p)}{2\sigma_m + \sigma_p - 2\Phi(\sigma_m - \sigma_p)} \tag{2.23}$$

$$C_1 = C_{el} \frac{2\varepsilon_m + \varepsilon_p - 2\Phi(\varepsilon_m - \varepsilon_p)}{2\varepsilon_m + \varepsilon_p + \Phi(\varepsilon_m - \varepsilon_p)} \tag{2.24}$$

$$C_2 = \frac{\Delta\varepsilon A}{h} \tag{2.25}$$

$$R_2 = \frac{\tau}{C_2} \tag{2.26}$$

2.1.4 Simulations

Now a complete equivalent circuit model is constructed with corresponding equation. It is time to put it to work and feed it some numbers. The channel dimension, which are required variables for the simulation, are matched to the dimension of the microfluidic chip used in this project. The electrolyte to be simulated is phosphate buffered saline (PBS). PBS is a water based electrolyte which is similar with respect to osmolarity and ion concentration to body fluids of mammals. The material for the beads is polystyrene. Table 2.1 gives typical values used in the simulations.

Table 2.1: Dimensions and electrolyte properties used in simulation.

Item		
Parameter	Symbol	Value
Channel height	h	20 µm
Channel width	w	50 µm
Electrode length	l	20 µm
Sample volume	hwl	20 pl
Bead diameter	d	3 µm
Bead volume	$\frac{4}{3}\pi(\frac{d}{2})^3$	14.14 fl
Electrolyte permittivity	ε_m	$80\varepsilon_0$ F/m
Electrolyte conductivity	σ_m	1.4 S/m
Bead permittivity	ε_p	$2.6\varepsilon_0$ F/m
Bead conductivity	σ_p	10×10^{-14} S/m

The values given in table 2.1 are used to calculate the values of the circuit elements, which represent Z_{sample}. The circuits are drawn with the component values next to the components (Fig. 2.7 and 2.8). It is clear from the values of R_2 and C_2 that they do not play a role in the system described by the values in table 2.1. The parallel combination of R_{el} and C_{el} has a cut-off frequency around 300 MHz, this is the same for the parallel combination R_1 and C_1. In both scenarios, with a bead and without a bead, the impedance of Z_{sample} is dominated by R_{el} or R_1 for frequencies well below 300 MHz.

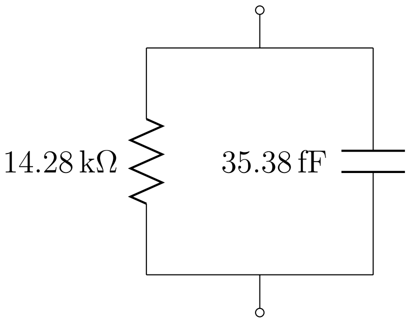

Figure 2.7: Z_{sample} without bead

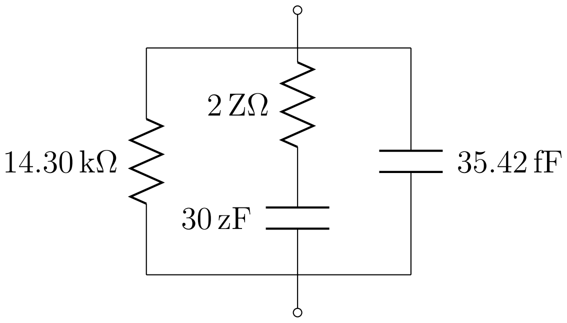

Figure 2.8: Z_{sample} with bead

Equation 2.23 shows that R_1 can be expressed in R_{el} times a factor. This factor is interesting as it indicates the difference between a sample volume with a bead and without a bead. The impedance of the sample volume should not change if there is a very small bead or if the conductivity of the bead is the same as that of the electrolyte. In fig. 2.9 this behaviour can be observed. For very small bead radii, this factor stays at one and is independent of conductivity of the electrolyte. At a conductivity of 1.4 S/m, the same as the electrolyte, the factor stays at one and is not influenced by the bead size. For bead conductivities smaller than the electrolyte conductivity, the impedance of the mixture increases. If the bead conductivity is larger the impedance decreases.

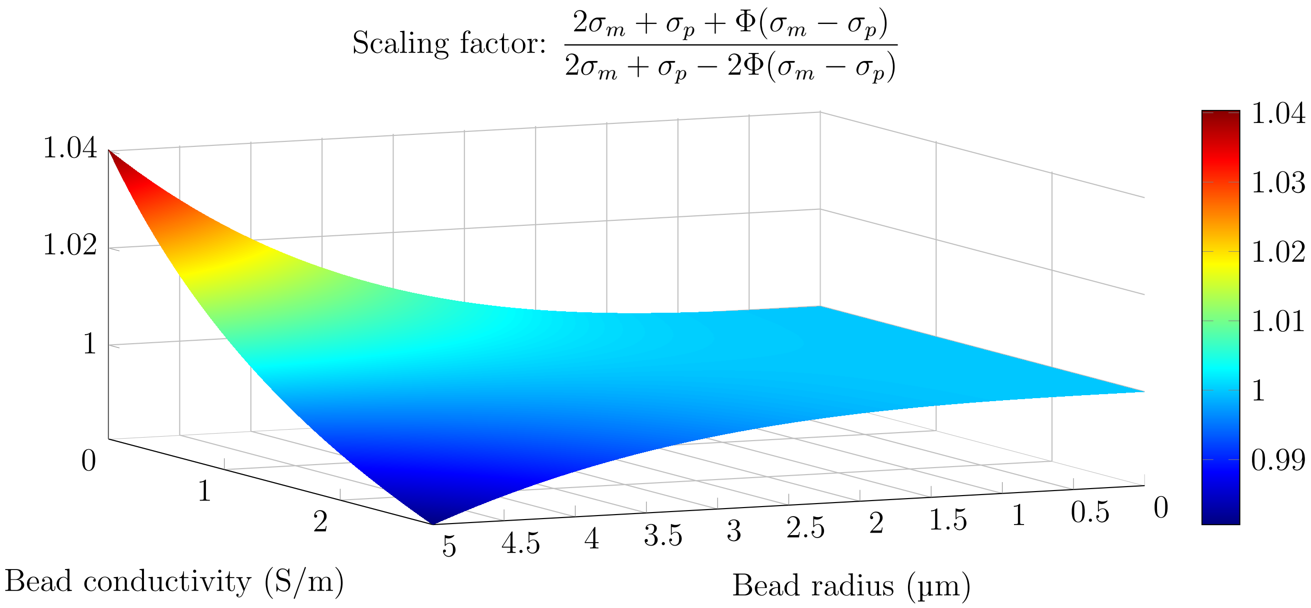

Figure 2.9: Scaling factor between R_1 and R_{el} when varying bead size and conductivity.

In graph 2.9 it can be observed that the change in Z_{sample} for a 3 µm bead is smaller than 1%. The change for a 3 µm polystyrene bead is more in the order of 0.1 % for the system described in table 2.1. To obtain good measurements of Z_{sample}, it is important that Z_{sample} dominates the behaviour of the total equivalent circuit(Fig. 2.4). Before anything can be said about the behaviour of the total equivalent circuit, all circuit elements need to have their values. The double layer capacitor is assumed to be dominated by the Helmholtz capacitance as the electrolyte has a high concentrations of ions. The range for the double layer capacitor is typically between 10 µF/cm^2 and 40 µF/cm^2 [4]. In this simulation is chosen to use a double layer capacitance of 15 µF/cm^2 and a parasitic capacitance of 1 pF.

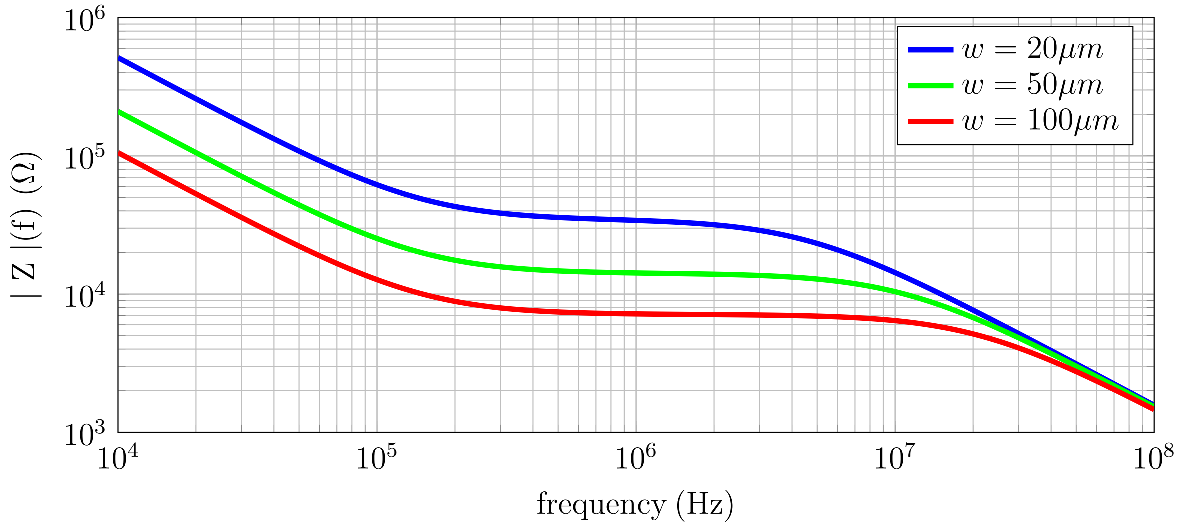

Figure 2.10: Impedance of the equivalent circuit for three different channel widths.

At low frequencies the behaviour of the equivalent circuit will be determined by the double layer capacitance (Fig. 2.10). From the point where the reactance of the double layer capacitor gets smaller than Z_{sample} the resistive plateau will start. Within the resistive plateau, the behaviour of the equivalent circuit is mostly determined by Z_{sample}. As the frequency increases even more, the reactance of the parasitic capacitor will become smaller than Z_{sample} and it will be the dominating factor. The start and end frequency of the resistive plateau can be estimated by equation 2.27 and 2.28 when R_{el} dominates Z_{sample} .

$$f_{start} \approx \frac{1}{2\pi R_{el} C_{dl}} \tag{2.27}$$

$$f_{end} \approx \frac{1}{2\pi R_{el} C_{par}} \tag{2.28}$$

The start of the resistive plateau seems to be at the same frequency for all three channel widths (Fig. 2.10). This is because the double layer capacitance increases with electrode area, whereas R_{el} drops with an increase in electrode area. Keeping their product in equation 2.27 constant. This frequency would however shift if one of the following parameters is changed: electrode surface roughness, channel height or electrolyte conductivity. The resistive plateau for the channel width of 20 µm is the smallest, due to the larger R_{el}. For all three cases, a measurement frequency of 1 MHz is very suitable for bead detection, since Z_{sample} dominates the behaviour of the equivalent circuit.

Table 2.2: Results of simulation at 1 MHz for 3 µm and 4 µm beads.

Channel width	Impedance	Scaling 3 µm	Scaling 4 µm	Peak 3 µm	Peak 4 µm
20 µm	34 157 Ω	0.27 %	0.63 %	92.2 Ω	215 Ω
50 µm	14 219 Ω	0.11 %	0.25 %	15.6 Ω	35.5 Ω
100 µm	7188 Ω	0.05 %	0.13 %	3.6 Ω	9.3 Ω

Table 2.2 shows the simulation of the impedance of 3 µm and 4 µm beads in a channel with a width of 20 µm, 50 µm and 100 µm. The reported impedance is the absolute impedance of the total equivalent circuit without a bead in the sample volume. The scaling factor gives the percentual change in R_{el} if a bead enters the sample volume. The last two columns give the height of the peak that corresponds with a bead flowing between the electrodes. The scaling factor is inversely proportional to the width of the channel. This is due to the smaller volume ratio between the bead and sample volume. The simulation predicts that the difference in peak height between 3 µm and 4 µm beads is a little more than a factor of 2. The system should be able to make a distinction between 3 µm and 4 µm beads based on the peak height detected as the beads flow between the electrodes.

2.2 Dielectrophoresis

Dielectrophoresis is used for the seperation of the different beads. This separation is controlled actively by turning the sorting electrodes on and off. The force generated by the dielectrophoresis should push the bead into a different flow lamina. When the main channel splits into two separate channels, the beads will be separated as they lie in in different flow lamina. The electrode configuration on the existing microfluidic chip is shown in fig. 2.11.

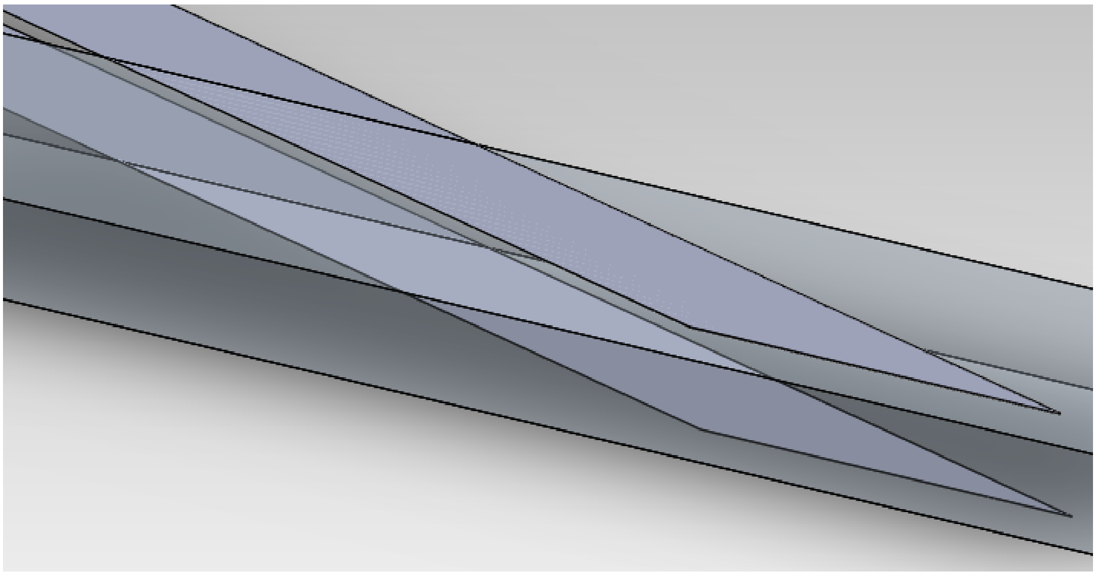

Figure 2.11: Sorting electrodes placed under an angle with the channel wall

2.2.1 Working principle

Dielectrophoresis is closely related to electrophoresis. The latter of the two involves the movement of a charged particle in an electric field, whereas dielectrophoresis involves the movement of polarizable particles in non-uniform fields.

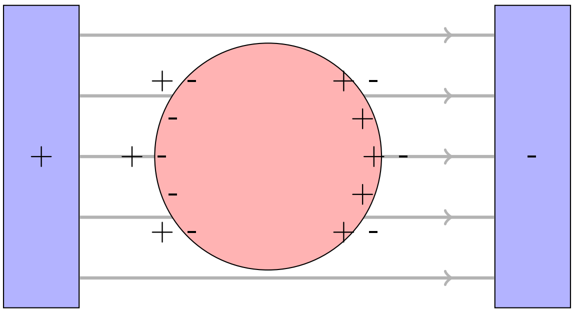

Figure 2.12: Surface charge on particle with higher polarizability then the medium.

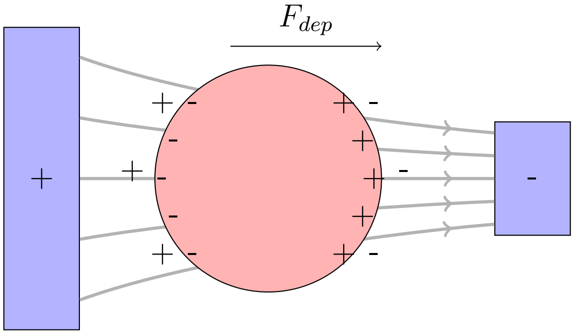

Figure 2.13: DEP force in non-uniform field

Within a electric field, the medium as well as the particle polarizes. When the medium and the particle do not have an equal polarizability, a net charge will form at the surface between them (Fig. 2.12). The amount of surface charge that forms on both sides of the particle will be the same, although it will differ in sign. The particle will not move in a homogeneous electric field, because the net force exerted on the particle will be zero. In a non- uniform field this is not the case (Fig. 2.13). The net surface charge which lies in the region where the electric field is higher(right side of the sphere), is subjected to a higher force. Now there is a net force on the particle and it will start to move. Equation 2.29 describes the time-average DEP force acting on a lossy homogeneous spherical particle [3].

$$\mathbf{F}_{DEP} = 2\pi\varepsilon_m r^3 Re[\tilde{f}_{CM}](\nabla\mathbf{E}^2) \tag{2.29}$$

$$\tilde{f}_{CM} = \frac{\tilde{\varepsilon}_p - \tilde{\varepsilon}_m}{\tilde{\varepsilon}_p + 2\tilde{\varepsilon}_m} \tag{2.30}$$

where ε_m is the permittivity of the medium surrounding the particle, r the radius of the particle, $Re[\tilde{f}_{CM}]$ the real part of the Claussius-Mossotti factor as given in equation. 2.30, E the rms amplitude of the electric field and finally ∇ the gradient operator. Equation 2.29 is derived based on a force that is exerted on a dipole. The electric dipole moment for two point charges of opposite sign separated by distance d is given in equation 2.31.

$$\mathbf{p} = q\mathbf{d} \tag{2.31}$$

The force on this dipole is expressed in equation 2.32

$$\mathbf{F}_{dipole} = q\mathbf{E}(x+d) - q\mathbf{E}(x) \tag{2.32}$$

If the dipole is small with respect to changes in the electric field, the force on the dipole can be approximated by equation 2.33

$$\mathbf{F}_{dipole} = (\mathbf{p}\cdot\nabla)\mathbf{E} \tag{2.33}$$

For a homogeneous sphere with conduction, the dipole moment can be described by equation 2.34[5].

$$\mathbf{p} = 4\pi\varepsilon_m \tilde{f}_{CM} R^3 \mathbf{E} \tag{2.34}$$

$$\mathbf{F}_{dipole} = \frac{1}{2} Re[(\mathbf{p}\cdot\nabla)\mathbf{E}^*] \tag{2.35}$$

In a real system with lossy medium and particle, a sinusoidal electric field will result in a phase difference between the dipole and the electric field. Therefore, equation 2.35 is used to calculate the time averaged value of the force[5]. Combining equation 2.35 with equation. 2.34 gives equation 2.29

2.2.2 Clausius Mossotti factor

The Clausius Mossotti factor is an important factor in the DEP force equation (eq. 2.29). If this factor is negative the particle will experience nDEP meaning the particle is repelled from regions where the electric field is high. A positive value will give pDEP, here the particle is attracted to regions where the electric field is high. The equation for the Clausius Mossotti factor is shown again in equation 2.30. Where $\tilde{\varepsilon}_p$ stands for the complex permittivity of the particle and $\tilde{\varepsilon}_m$ for the complex permittivity of the medium. This complex permittivity is expressed as: $\tilde{\varepsilon}_i = \varepsilon_0\varepsilon_i - \frac{j\sigma_i}{\omega}$, which also includes the conductivity and is therefore frequency dependent . The real part of this factor always has a value between between -0.5 ($\tilde{\varepsilon}_p << \tilde{\varepsilon}_m$) and 1 ($\tilde{\varepsilon}_p >> \tilde{\varepsilon}_m$). At low frequencies the conductivity of both the medium and the particle determines the Clausius Mossotti factor, while at higher frequencies the Claussius Mossotti factor is determined by the permittivity (Fig. 2.14).

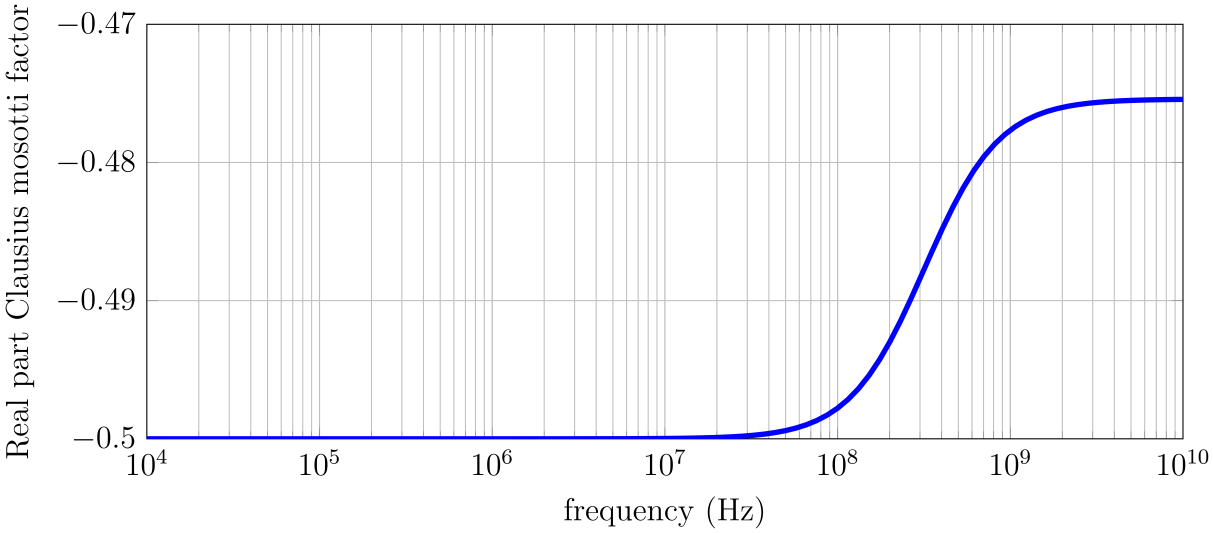

Figure 2.14: Claussius Mossotti factor over frequency, parameters used a given in table 2.1.

2.2.3 Flow profile

The Navier-Stokes equation describes the motion of fluids. This equation is a complex non-linear differential equation which can be used to determine the flow profile within the microfluidic channel. First some conditions that simplify the full Navier-Stokes equation. The flow of interest is pressure driven and is in a steady state. The fluid of interest is incompressible. The channel on the microfluidic chip has a rectangular cross section. This rectangular cross section is placed on the yz-plane with the fluid flow solely in the x-direction. This results in a flow velocity field as given in equation 2.36.

$$\mathbf{v}(\mathbf{r}) = v_x(y,z)\mathbf{e_x} \tag{2.36}$$

Equation 2.37 gives the Navier-Stokes equation for the assumptions given above[6].

$$[\partial_y^2 + \partial_z^2]v_x(y,z) = -\frac{\Delta p}{\eta L}, \qquad \text{for } -\frac{1}{2}w < y < \frac{1}{2}w,\ 0 < z < h \tag{2.37}$$

$$v_x(y,z) = 0, \qquad \text{for } y = \pm\frac{1}{2}w,\ z = 0,\ z = h \tag{2.38}$$

With the boundary conditions provided by equation 2.38, the solution to this differential equation is a Fourier series as shown in equation 2.39 [6].

$$v_x(y,z) = \frac{4h^2\Delta p}{\pi^3\eta L}\sum_{n,odd}^{\infty}\frac{1}{n^3}\left[1 - \frac{cosh(n\pi\frac{y}{h})}{cosh(n\pi\frac{w}{2h})}\right] sin\left(n\pi\frac{z}{h}\right) \tag{2.39}$$

In this equation h is the height of the channel, Δp the pressure drop over the channel, η the viscosity of the fluid and L the length of the channel. An approximation of $v_x(y,z)$, where the first 50 terms of the series are calculated, is shown in fig. 2.15.

The beads carried by the electrolyte flow have the same velocity as the electrolyte. If an external force is exerted on the polystyrene bead, e.g a DEP force, the beads velocity will change, resulting in a velocity difference between the electrolyte flow and the bead. The bead will now experience a stokes drag from the electrolyte. The force exerted on a sphere by this stokes drag is given in equation 2.40.

$$\mathbf{F}_d = 6\pi\eta r\mathbf{v} \tag{2.40}$$

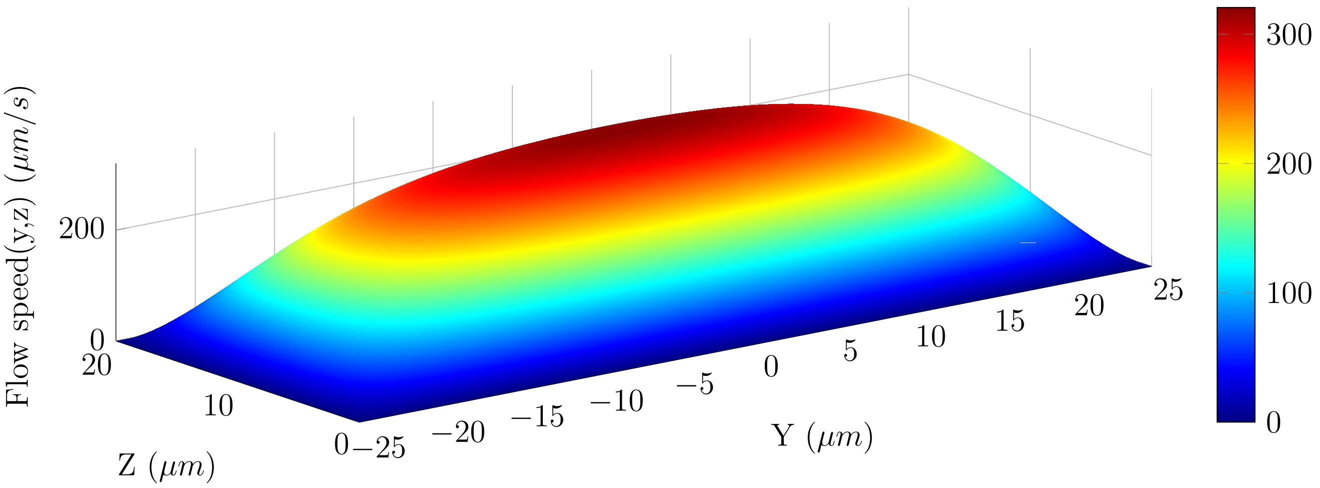

Figure 2.15: Flow velocity for a 0.01 µl/min flow rate in a rectangular channel.

where η is the dynamic viscosity of the fluid, r is the radius of the sphere and $\mathbf{v}$ the velocity difference between the fluid and the sphere. The balance between the DEP-force and the Stokes drag force will determine the movement of the the bead.

Chapter 3

Materials and Methods

3.1 Device design and fabrication

In this section, a summary is given of the important parts and the fabrication processes of the microfluidic devices used in this project. Figure 3.1 shows what the chip looks like.

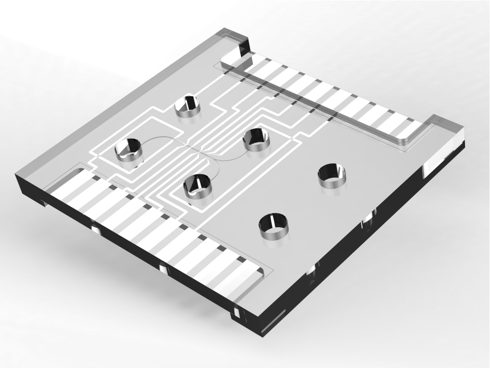

Figure 3.1: Solidworks render of the whole chip.

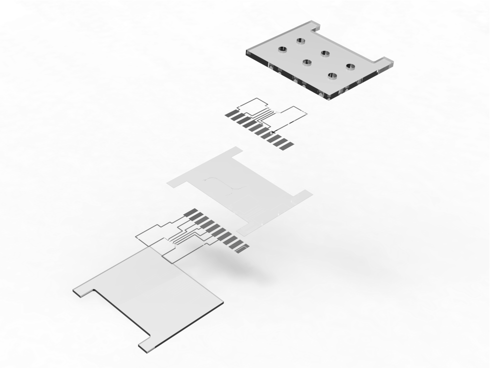

Figure 3.2: Exploded view of the chip.

The parts of which this chip is made, are shown in fig. 3.2. The bottom part of the microfluidic device is a 500 µm thick part of borofloat glass with a dimension of 18 mm × 20 mm. Platinum micro electrodes are embedded in the glass. The middle part of the device is a 20 µm thick layer of PerMX3020 (Dupont). This is an important layer as it contains the microfluidic channels. Platinum micro electrodes above the PerMX3020 layer are again embedded in the top glass part, which is 1100 µm thick. Electrical connections to the micro electrodes are made via large electrode pads. These pads can be reached through holes that are powder blasted into the glass parts. The holes for the microfluidic connections and electrical connection are always designed in the same place. This way the same chip holder can be used for all the chips, while still varying channel and electrode layout.

The parts of the microfluidic chip are produced in a cleanroom with a lithographic patterning process. In total five lithographic masks are needed to make all the features on the chip (Fig. 3.3). A whole wafer is processed at a time with a final step of dicing out 12 individual chips. A simplification of the process flow for the different parts of the chip is shown in figures 3.3 and 3.4

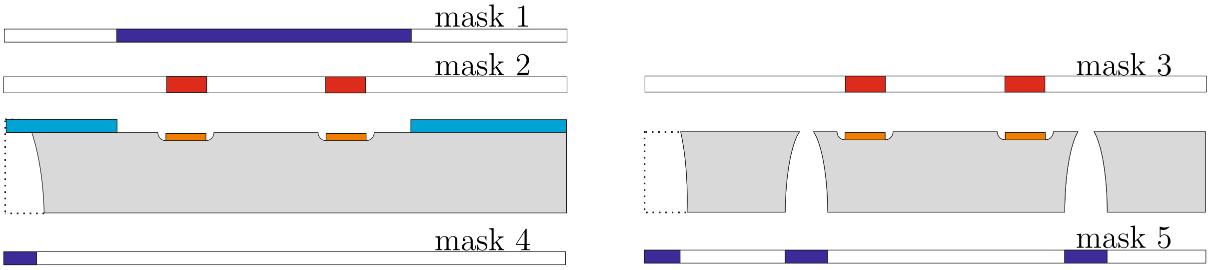

Figure 3.3: Masks and wafers after processing (left:bottom wafer, right:top wafer).

Bottom borofloat glass wafer

- Align mask 2 and expose photo resist
- Develop photo resist
- Etch room for micro electrodes
- Sputter 30 nm of Tantalum
- Sputter 120 nm of Platinum
- Pattern micro electrodes with liftoff process
- Laminate both sides with powder blast resist
- Align mask 4 and expose powder blast resist
- Develop powder blast resist
- Powder blast access window to electrodes
- Remove powder blast resist and clean
- Laminate PerMX3020 foil
- Align mask 1 and expose foil
- Develop channels in foil

Top borofloat glass wafer

- Align mask 3 and expose photo resist
- Develop photo resist
- Etch room for micro electrodes
- Sputter 30 nm of Tantalum
- Sputter 120 nm of Platinum
- Pattern micro electrodes with liftoff process
- Laminate both sides with powder blast resist
- Align mask 5 and expose powder blast resist
- Develop powder blast resist
- Powder blast holes and access window to electrodes
- Remove powder blast resist and clean

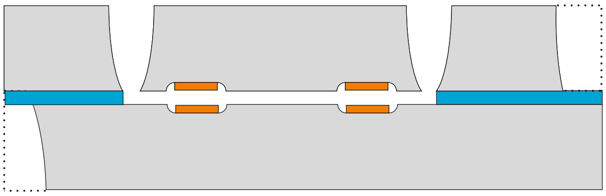

Figure 3.4: Bonded chip

Bonding top and bottom wafer

- Align top and bottom wafer
- Bond top and bottom wafer
- Dice out the twelve individual chips

3.2 The setup

Besides the microfluidic chip a lot of instrumentation is required to perform electrical measurements. A summery of devices used during this project is shown in figure 3.5. The microscope gives visual feedback on what is happening inside the chip and can be used to correlate between visual and electrical events, e.g a bead passing the electrodes. For impedance measurements the impedance spectroscope or the capacitance bridge can be used. The function generator is used to generate an electric field within the microfluidic channesl using the DEP electrodes. Finally the syringe pump provides the fluidic flow within the chip.

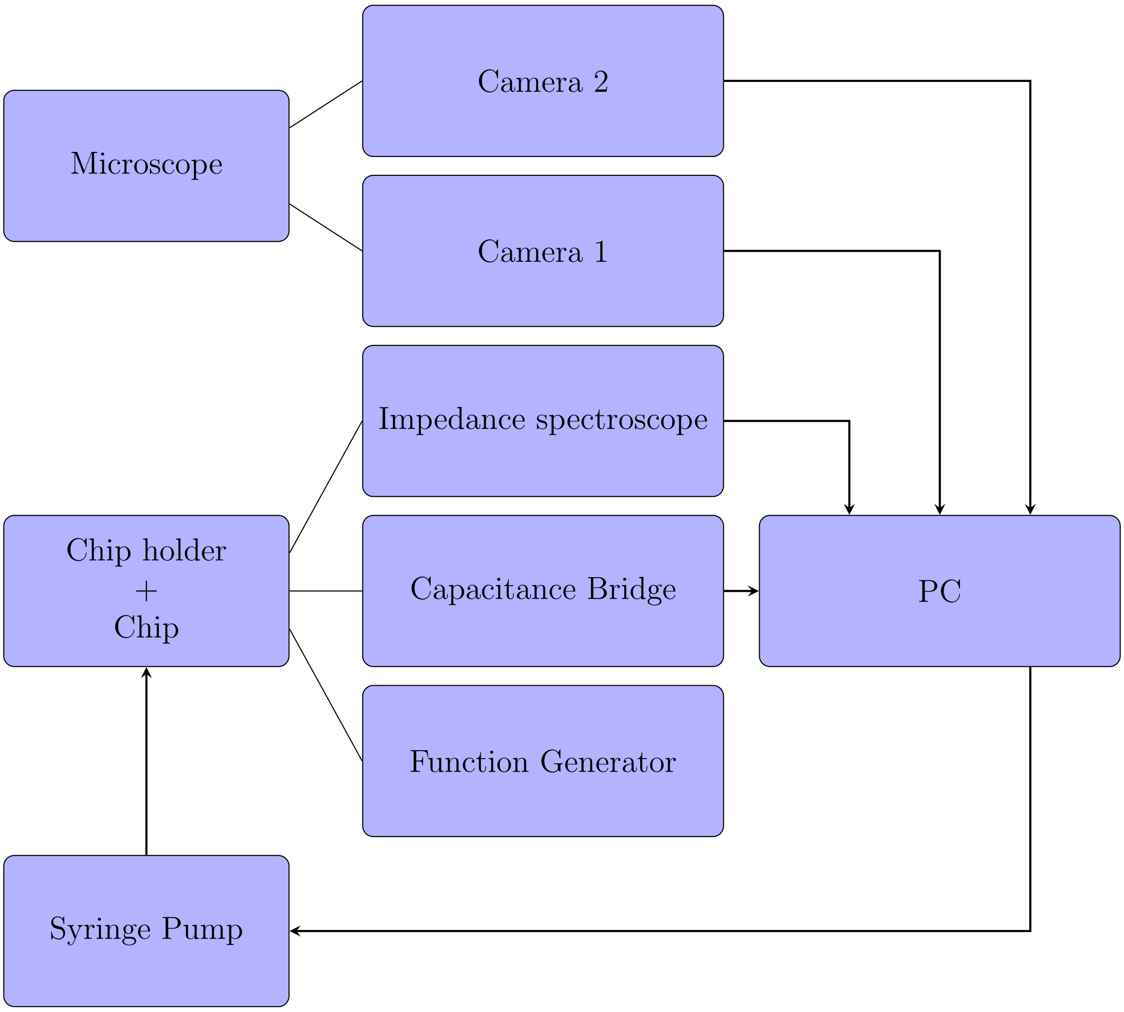

Figure 3.5: Summery of devices used during this project.

Almost all devices are connected to the pc, which is used to collect data. This data is used to characterize the different parts of the microfluidic device. In a later stage of the project the PC is also used as a controller to actively control the sorting electrodes. Detailed information on the devices used can be found in table 3.1.

Table 3.1: Detailed information of the devices used during the project.

Device	Manufacturer and type	Serial
Microscope	Nikon TE2000-E	-
Camera 1	Nikon DS-Ri1 + DS-U3	-
Camera 2	Basler acA780-75gc	-
Chip holder	BIOS made	-
Impedance spectroscope	Zurich Instruments HF2IS	IS-DEV91
Current amplifier	Zurich instruments HF2TA	TA-DEV70
Capacitance bridge	Andeen Hagerling AH2700A	00700356
Fucntion generator	Agilent 33220A	MY44036289
Syringe Pump	NEMESYS low pressure syringe pump	-
PC	Dell Optiplex 9010	-

3.3 Data acquisition and control with Labview

As mentioned in the previous section, a PC is used to collect data from the measurement devices. In a later stage of the project the PC is used to control when the sorting electrodes should be turned on. To make this happen of course software is needed. Almost all devices used have their own software to record measured data, but it is hard to start a measurement at the same time to synchronize between different devices. Making software of the different manufactures talk to each other would be very hard. Therefore, it was decided that it would be best to build new software. With this new software is should be possible to activate a measurement and synchronously record data from multiple devices in the setup. Synchronized data will make data processing much easier as time information can be used to link events together.

3.3.1 Why Labview?

The main reason Labview was chosen for this project is that a lot of the devices in the setup already have drivers for Labview. These drivers take care of the low level communication between Labview and the measurement device. They also provide the programmer high-level functions which control the measurement device. With high-level functions it is possible to write software relatively fast, because the communication with the device is already taken care of. A slight drawback of these drivers is that synchronization will not be optimal, because the time sensitive communication is hidden from the programmer. Together with a non-realtime operating system as Windows 7, timing will never be perfect, but offers a great advantage over manual activation. However, Labview together with the device drivers provides a platform where fast development of software is possible.

Unfortunately, no drivers where found for the Nikon camera, so it can not be used in the Labview software. For the Basler camera, Zurich impedance spectroscope, Andeen Hagerling capacitance bridge, the Nemesys syringe pump and the Agilent function generator, drivers are available and can be use in Labview.

3.3.2 What needs to be controlled?

In the introduction the different functions of the microfluidic chip are summarized. The diagram from the introduction is drawn again here to show which parts need to be controlled by Labview software (Fig. 3.6). When the beads enter the chip they are first differentiated by the peak height of the impedance signal. Then, the beads are transported through the chip by the electrolyte flow. At a certain point in time, the beads will pass the separation electrodes, which should be turned on or off depending on the type of bead flowing by.

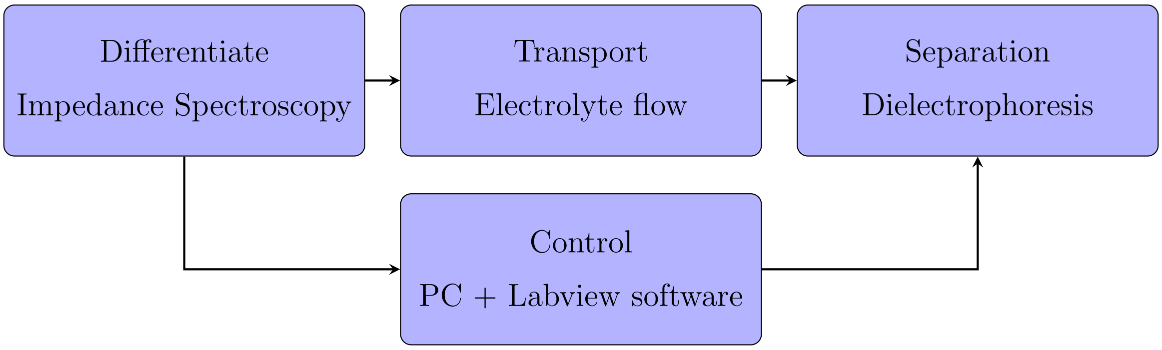

Figure 3.6: Functions of the microfluidic system.

The Labview software should perform the following actions in chronological order:

- Get impedance samples from Zurich impedance spectroscope
- Find peaks in impedance signal
- Categorize peak in 3 µm or 4 µm
- Wait for bead to travel to sorting area (fig. 3.7)
- Turn sorting electrode on/off, based on category of the bead

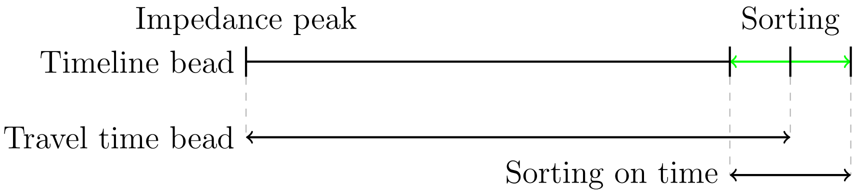

Figure 3.7: Timeline for bead travelling from the impedance electrodes to the sorting electrodes.

To perform the described action, the speed of the individual beads must be known. From theory it is known that the liquid flow close to the wall is slower than in the middle of the channel. This is why an average flow speed can not be used to calculate the travel time of the bead. The impedance electrodes have a certain width and the bead is between them for a certain time. This combination gives speed information, which is enclosed within the impedance signal. The speed information can be extracted by analysis of the peak width. This measurement approach to determine the bead velocity will have a certain accuracy and therefore the sorting electrodes will have to be actuated for some time, to be sure that the bead passes the electrodes when they are actuated.

3.3.3 Labview program

The program roughly consist out of the blocks drawn in figure 3.8. At start up, the main initialization will enable the blocks of the devices that are selected in the user interface. Every device block consists of some initialization code to get the device up and running. After the initialization, a while loop runs continuously, displaying the current measurement on the screen. The while loop continuously polls the user interface to see if settings of the device need to be changed and if the current measurement data should be saved to the hard drive of the PC. When a measurement is started the settings are locked and can not be changed until the measurement is stopped. Furthermore, a new file is automatically generated. The code for the file interaction is included in the while loop of the camera, since this part of the software is always running. Otherwise the software of the manufacturer of the device is a better choice if stand alone measurements needs to be done. Due to time constrains the control part of the software runs inside the while loop of the impedance spectroscope and is thus also only available for the Zurich HF2IS.

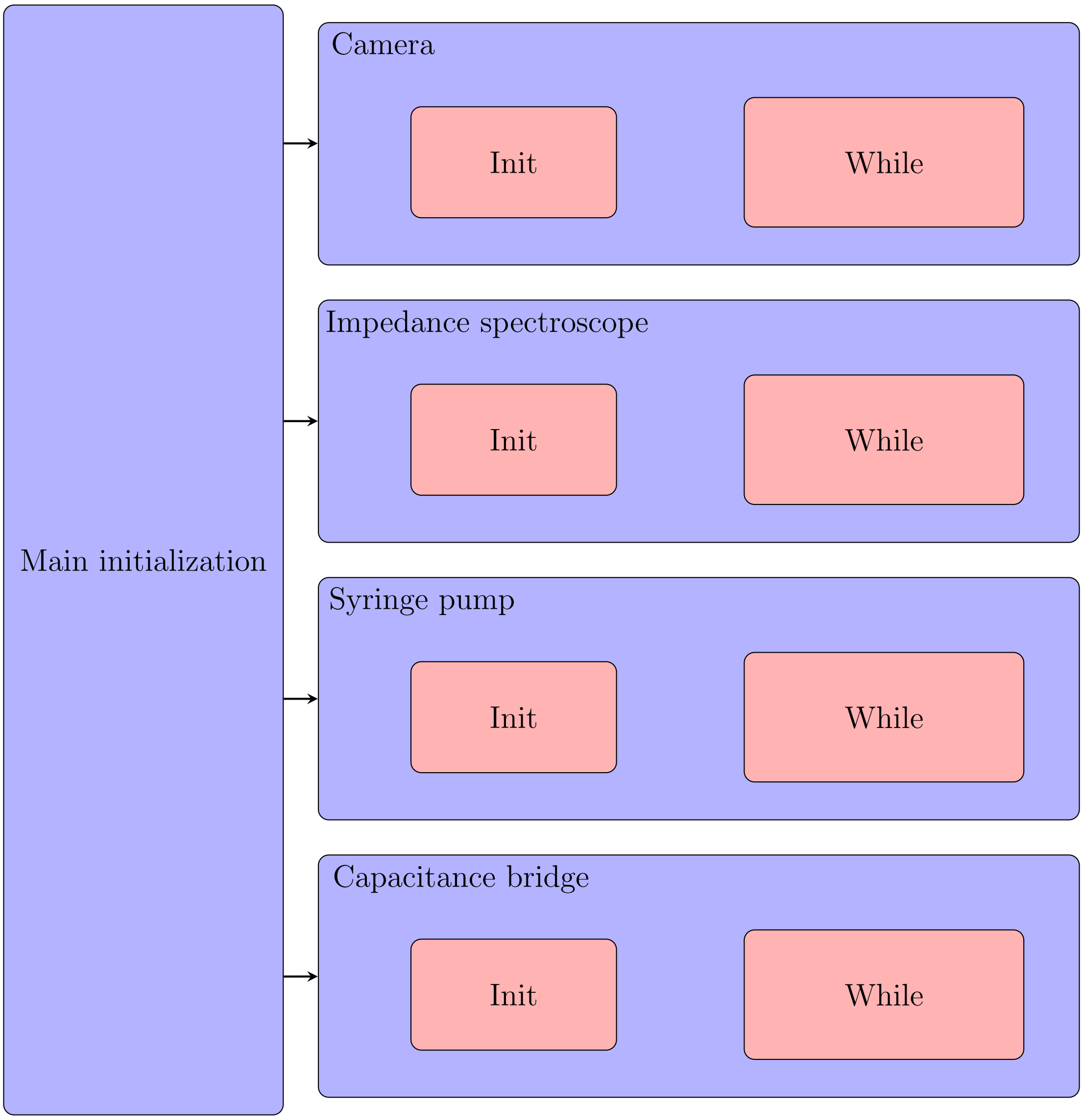

Figure 3.8: Organization of Labview software

Camera

The Basler camera is connected to the PC using a Gigabit Ethernet connection. The camera communicates using the GigE Vision protocol. Labview has a driver called IMAQdx, which is included in the NI vision acquisition software package. This driver supports all GigE Vision cameras, takes care of all low level communication with the camera and has an internal buffer for the video frames. In this application the camera takes care of the timing between the frames itself. Therefore, it is important that no frames are lost, because this would result in bad synchronization between data of the different devices. During the initialization the internal frame buffer of the IMAQdx driver is set to 500 frames and it is set to give an error when a frame is overwritten before it is read. The frames are read from the driver and then displayed in the user interface. When a measurement is running the frames are cut by the region of interest chosen in the user interface before they are saved. This helps to reduce file sizes, as the movies are saved in an uncompressed video format. The uncompressed video was chosen for two reasons: to unload the CPU during a measurement and to prevent quality lost before post processing the file.

Impedance spectroscope

The Zurich Instruments HF2IS impedance spectroscope is connected to the PC using a USB connection. The software provided by the manufacturer exist out of two parts, ZiBase and ZiControl. They can be seen as a server and client combination. Zurich provides a Labview virtual instrument (VI) as a driver, which is used in the Labview program to communicate with ZiBase. ZiBase is responsible for the low level communication over the USB bus and holds a buffer with samples received from the impedance spectroscope. In the initialization, the Labview program subscribes itself to the channels of interest. In this case, channel 1 is used for the current measurement and channel 2 is used for the voltage measurement. In the while loop the measurement data of the subscribed channels is polled. Then samples from the current and voltage channel are synchronized using the timestamp of each sample. The synchronized current and voltage samples are then used to calculate the impedance (eq. 3.1). The impedance spectroscope returns an in phase component and na out of phase and therfore component complex numbers are used to do the calculation.

$$\tilde{Z} = \frac{\tilde{U}}{\tilde{I}} \tag{3.1}$$

$$\tilde{U} = U_{\text{In phase}} + U_{\text{Out of phase}} j \tag{3.2}$$

$$\tilde{I} = I_{\text{In phase}} + I_{\text{Out of phase}} j \tag{3.3}$$

The absolute value and the phase of the impedance are then plotted in the user interface. The impedance data together with the corresponding time stamps is passed to the peak detection module. During this project, two different peak detection methods were designed. These methods are explained in the following two paragraphs.

The first peak detector uses a second order butterworth high pass filter with a -3dB point of 0.25Hz. This filter is intended to filter out the offset and slow moving drift of the impedance signal, without losing any peak data. A peak is detected when the output of the filter exceeds a certain noise threshold. Then impedance samples with corresponding timestamps are stored as long as the output of the filter exceeds the threshold. As soon as the output of the filter drops below the threshold, storage of samples stops and the whole peak is in memory. The following parameters of the passing bead are extracted from the peak data. The sample with the highest value is recorded as the peak height. When the peak height is within the window of interest(minimum and maximum threshold), a flag is set that the bead should be sorted. The speed of the bead is determined by the time the filtered impedance signal exceeds the noise threshold. This speed is then used to calculate the travelling time of the bead between the impedance electrodes and the sorting electrodes. The bead velocity and the measurement inaccuracy together determine the duration of the electrode activation. The final output of the peak detector contains the following information: time of peak detection, bead speed, peak height, time at sorting electrode, sort? (yes/no),the timestamp of the sorting electrode switching on and the timestamp of the sorting electrode switching off. The peak detector holds this information for the last 12 beads.

The second peak detector will only detect peaks with a certain shape [7]. The peak detector functions by constantly fitting a peak template to the impedance signal. The peak consist of several measured samples, so all incoming impedance samples together with their timestamps are stored in a buffer of 200 samples. Hundred samples in the middle of this buffer are used to fit the template to. The peaks have different heights and there is a slight drift in the impedance signal, therefore the template needs to be scaled and set to a certain offset (eq. 3.4 [7]). The scaling and offset of the template minimize the fitting error.

$$\text{Fitted\_Template} = \text{Template} * \text{Scale} + \text{Offset} \tag{3.4}$$

$$\text{Scale} = \frac{\sum(\text{Template} * \text{Data}) - \sum \text{Template} * \sum \text{Data}/N}{\sum \text{Template}^2 - \sum \text{Template} * \sum \text{Template}/N} \tag{3.5}$$

$$\text{Offset} = \frac{\sum \text{Data} - \text{Scale} * \sum \text{Template}}{N} \tag{3.6}$$

$$\text{Standard\_Error} = \sqrt{\frac{SSE}{N-1}} \tag{3.7}$$

$$\text{Detection\_Critereon} = \frac{\text{Scale}}{\text{Standard\_Error}} \tag{3.8}$$

Equations 3.5 and 3.6 are derived by minimizing the squared errors between the data and the fitted_template, the complete derivation can be found in [7]. The equations above need to be recalculated for every new sample that comes into the buffer. A peak is detected if the detection_creterion (eq. 3.8) passes a threshold. This happens if the scale is large and the error of the fit between the template and the data is small.

If a peak is detected, the whole input buffer is copied since it hold the samples the peak consists off. The copy of the peak samples is used to find the peak height and the speed of the bead. The sample with the lowest value will be subtracted from all samples in the buffer to remove the offset. The maximum value will now represent the peak height. To obtain speed data, the time between the inflection points of the peak needs to be determined. The peak samples also hold noise, therefore a fit is made to the peak. With this fit a smooth peak shape can be obtain to find the inflection points. A trail and error approach showed best shape agreement between the fit and the peak samples for a Gaussian fit. The second peak detector uses the peak height and the speed in the same way as the first peak detector to calculate bead parameters and stores these for the last 12 beads detected.

In the while loop, a continuous check is performed to see if one of the 12 beads outputted by the peak detector is currently at the sorting electrodes. This is done by comparing the timestamp of the latest impedance sample received, with the timestamps given to each bead for switching the sorting electrode on or off. If one or more beads are currently at the sorting electrodes, the electrodes should be turned on, but only if all beads have their sort? flag set. This makes sure only beads of interests are deflected.

Syringe pump

The Memesys syringe pump is connected to the pc using a USB connection. The manufacture also provides VI's which can be used in Labview; they provided access to the device with high level functions. The initialization code will load syringe info from a file, which is also used by the software of the manufacturer. This way new syringes only have to be programmed once. This info will be loaded in the user interface. The while loop waits on the user to give a command which it will then communicate to the pump. When running a measurement, the flow rate is saved to a file every half second.

Capacitance bridge

The Andeen Hagerling capacitance bridge is connected to the PC using a serial to USB cable. The capacitance bridge can also be controlled by available VI's that take care of the low level communication with the device. During initialization the capacitance bridge is programmed to continuously take measurements. The units of the capacitance and loss output are set to pF and jpF, because these seem to give the fastest results. The while loop continuously takes the results in pF and jpF units and converts them to absolute impedance and phase, which are displayed in the user interface. When a measurement is running, the results and corresponding timestamp are also saved to a file.

3.4 Data processing with Matlab

Matlab is used to process impedance data as well as video data that is obtained with the setup. Within the recorded impedance data, the peaks of beads passing the impedance electrodes should be detected. The time the peak occurred and peak height should be recorded. In the video data the position of beads should be tracked. The position data should also hold time information. Finally, the peaks in the impedance data should be linked to beads in the video data, in order to correlate impedance and video data.

3.4.1 Impedance data

The first step in peak detection is the removal of drift and offset. A moving average filter is used to remove drift and offset. This is done by subtracting the averaged signal from the original. The input and output of the moving average filter are subtracted from each other, therefore it is important that there is no phase shift between them. This is achieved by using the buildin Matlab filter ”filtfilt”. The result of this subtraction is a signal centered around zero holding the peaks of the beads passing the electrodes. Subsequently, the peak height and time information is found by the buildin Matlab function ”findpeaks”. The ”findpeaks” function has a option to set the minimum peak height. The minimum peak height is used to prevent peak detection in the noise of the signal.

3.4.2 Video data

Video tracking of beads in a microfluidic channal is based on a Matlab example named: ”Motion-Based Multiple Object Tracking” [8]. This example is part of the Computer Vision System Toolbox. In figure 3.9, the flowchart of the script is illustrated. All frames of the video are processed one by one. In every frame, objects are detected by comparing the frame to a background model. The center position and area of the individual objects is determined. For every object found a attempt is made to assign it to a track. A kalman filter with a constant velocity model is used to predict the location of the object in the following frame. The predicted locations of the existing tracks are compared with the objects found. This results in three lists: objects assigned to a track, tracks that where unassigned and object that where unassigned. Objects, that were assigned to a track, are used to update the track. Unassigned tracks are deleted when they are unassigned for a consecutive number of frames. Objects that are not assigned to an existing track are assigned to a new track. Then the objects are annotated in the frame with a track id. The annotated frame is shown on screen.

Changes made to the example script are mostly done in the function ”Detection to assigned tracks”. A list is added besides the existing track list, where the position and time data of the objects is also saved. Entries in this list cannot be deleted by the script. The example script is also changed in a way that it saves the list with position data to a file. The annotated frames are also saved to a movie file.

3.4.3 Combining data

Information about the bead is of interest. The impedance data gives a peak height together with the time the peak occurred. The video data provides a set of positions and times per bead. To link the impedance data to the video data, the time at which the bead was at the impedance electrodes needs to be known. A polynomial fit of the third order is made to the set of positions and times. The fitted function gives the position of the bead over time. This function is used to calculate at which time the bead was present at the position of the impedance electrode. This

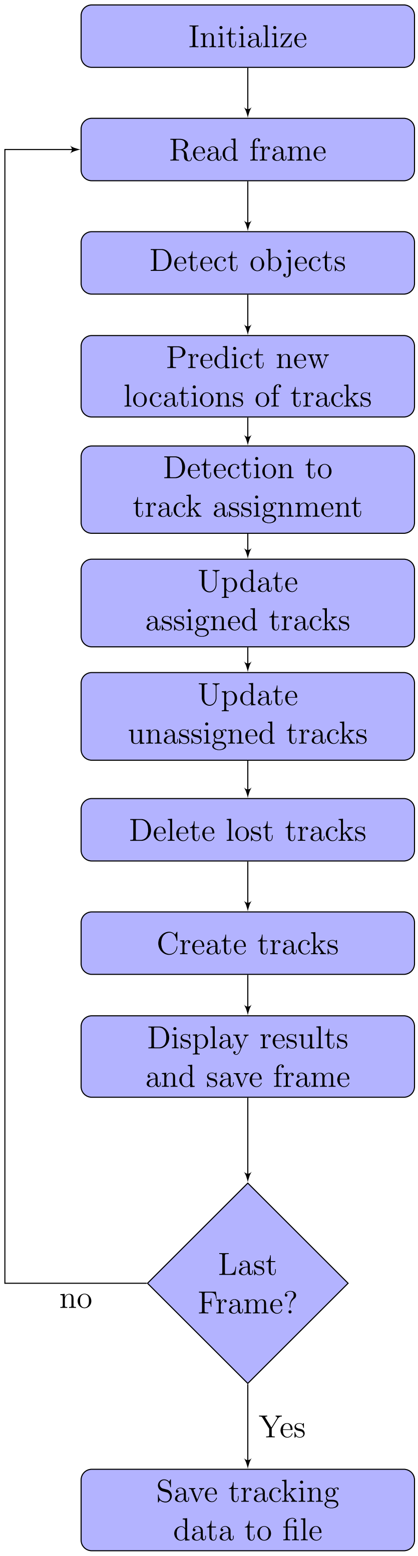

Figure 3.9: Flowchart indicating the main functions in the Matlab script used for video processing.

time should correspond to the time of the peak in the impedance data. With these times, the video data and impedance data of a bead can be linked. To obtain extra information the slope of the position function is determined at the time the bead passes the impedance electrodes. This slope gives the speed of the bead when it passes the impedance electrodes.

3.5 Measure protocols

Lets start with the materials. PBS was produced by soluting a two tablets in 400 ml demiwater. MQ with a resistivity of 18.0 MΩ/cm was produced by a Miliport Milli-Q Synthesis A10. The 3 µm beads were polybead dyed red microspheres from Polysciences with catalog number 17137. The 4 µm beads were microbead NIST traceable size standard from Polysciences with catalog number 64070. If a coating was used, it was applied by 100 µg/ml PEG-PLL solution in MQ. A 50 µl Hamiltion Gasthight 1705 syringe is used in all experiments.

3.5.1 Impedance measurements with AH2700A

All measurements with the Andeen Hagerling capacitance bridge were performed at 20 kHz. This is the maximum frequency at which the bridge can perform measurements. Averaging was set to 1 to obtain a high sample rate. The dimensions of the electrodes were 20 µm × 20 µm in a channel with a height of 20 µm. The 3 µm beads were diluted to a concentration of 2×10^6 beads/ml. The chip was coated with the PEG-PLL solution for a least 15 minutes. Flow conditions were varied between 0.002 µl/min to 0.05 µl/min. Measurements were performed by flowing the bead solution through the chip for 5 to 10 minutes. The impedance was recorded during this time period. The amplitude of the applied potential was 0.25 V. For drift and noise measurements, only PBS or MQ was flown through the chip. Measurement were taken at potentials of 0.1 V, 0.25 V and 0.5 V. For each potential, the flow was changed in the following steps 0.002 µl/min, 0.01 µl/min and 0.05 µl/min.

3.5.2 Impedance measurements with HF2IS

Impedance measurements with the Zurich HF2IS were performed in a four terminal configuration (Fig. 3.10). The current was amplified with the HF2TA with amplification factor of 1000. The separation between the current and voltage measurement was made close to the chip holder, so that the voltage measured represented the voltage applied over the fluidic channel. The dimensions of the electrodes were 20 µm × 20 µm in a channel with a height of 20 µm. Output 1 of the impedance spectroscope was set to apply a sinusoidal 1 MHz signal with an amplitude of 0.5 V. The bandwidth of the low pass filter in the Zurich was set to 19.9 Hz with a sample rate of 225 Hz. 3 µm and 4 µm beads suspensions in PBS were made with concentrations of 2×10^6 beads/ml. The suspensions were flushed through the chip with a flow rate of 0.01 µl/min. Measurements were performed by recording the impedance during a period of 5 to 10 minutes.

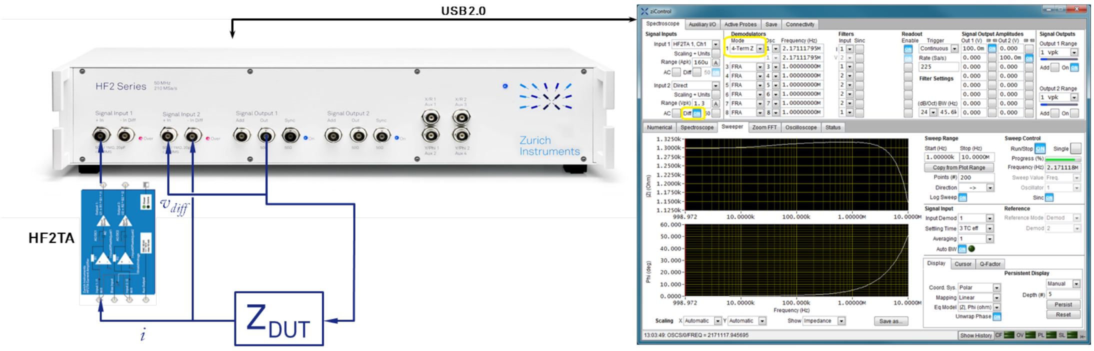

Figure 3.10: HF2IS device set up for a four terminal measurement[9].

3.5.3 Dielectrophoresis measurements

Dielectrophoresis measurements were performed using both the focusing part of the chip as well as the sorting part. The electric field was constantly applied by the Agilent function generator at a frequency of 10 MHz. The amplitude of the electric field was varied from 0.1 V to 2.5 V and finally 5 V. The measurements were performed at a flowrate of 0.01 µl/min and 0.025 µl/min. The dimensions of the channel cross section were 20 µm × 100 µm. Both 3 µm and 4 µm beads were suspended together in PBS, both with a concentration of 2×10^6 beads/ml resulting in a overall bead concentration of 4×10^6 beads/ml. Measurements were performed for 5 minutes after which the parameters where changed.

3.5.4 Combined Dielectrophoresis and Impedance measurements

The experiments described in this subsection were used to verify the working of the whole system. DEP was used to focus the beads prior to the impedance measurement. Subsequently, DEP was used to separate the beads. The experiment tested the influence of the DEP focusing on the impedance peak height and the influence of the active DEP sorting on the impedance measurement. Both were tested with the same chip layout with channel cross section of 20 µm × 50 µm. The focusing is also tested on a chip with channel cross section of 20 µm × 20 µm, using 3 µm beads suspended in PBS with a concentration of 4×10^6 beads/ml. While 3 µm and 4 µm beads suspended together in PBS, both with a concentration of 2×10^6 beads/ml resulting in a overall bead concentration of 4×10^6 beads/ml were used for the other experiments.

The impedance was measured with the HF2IS in a four terminal configuration. The current was amplified with the HF2TA with amplification factor of 1000. Output 1 of the impedance spectroscope was set to apply a sinusoidal 1 MHz signal with an amplitude of 0.5 V. The bandwidth of the low pass filter in the Zurich was set to 200 Hz with a sample rate of 899 Hz.

The electric field for the focusing electrodes is supplied by the Agilent function generator. The potential applied is a 10 MHz sinus with an amplitude of 1 V. The electric field for the sorting electrodes is applied on-demand by the second output of the Zurich. The amplitude and the frequency of the applied DEP potential are varied. The flow is set to 0.01 µl/min. Measurements are again about 5 to 10 minutes in length were the impedance is recorded.

Chapter 4

Results and Discussion

4.1 Impedance measurements

The function of the impedance measurements in the proposed system is to differentiate between beads with a size of 3 µm or 4 µm. The peak in the impedance signal that corresponds to a bead passing the impedance electrodes is used for this purpose. More specifically, the peak height is used to determine the size of the beads.

4.1.1 Drift and Noise

To detect peaks, a stable background signal is required. In practice, some drift and noise will always be present. In this subsection, the drift and noise of the impedance measurement of only the electrolyte is investigated. All measurements in this section are performed with the AH2700A.

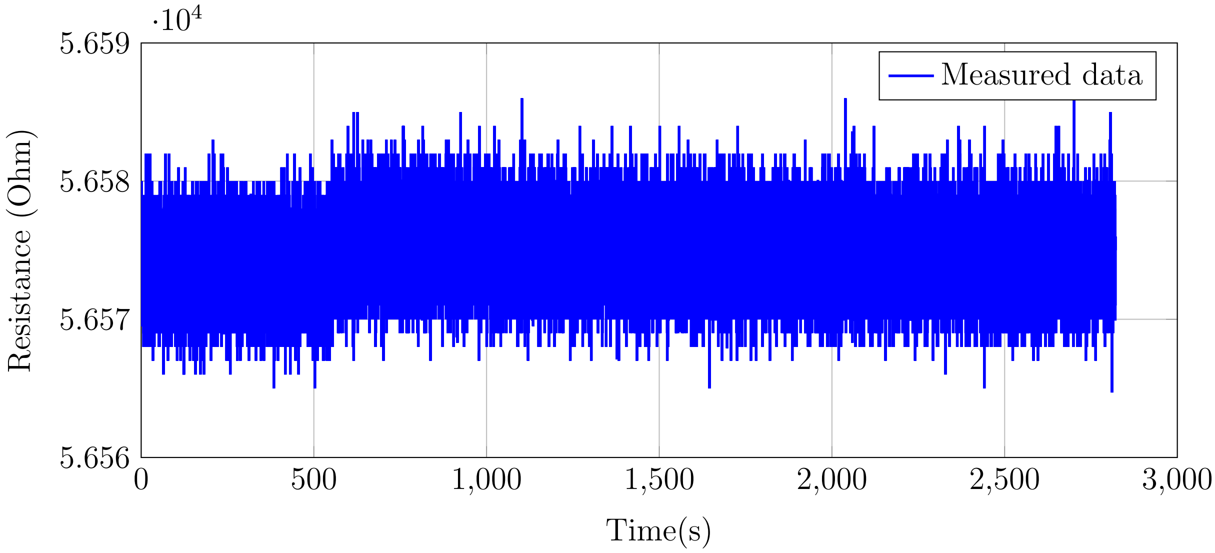

Figure 4.1: Long term drift in the real part of the impedance for a standard 56 kΩ resistor and a 50 pF capacitor in series. Measurement was performed at 20 kHz.

Figure 4.1 shows a measurement of a resistor in series with a capacitor. This measurement shows the long term stability of the measurement device and the setup. Over a period of 45 minutes, the real part of the impedance(resistance in a series configuration) had a negligible drift of a few Ω. The noise band was about 10 Ω, which was around 0.02 % of the total signal. From theory, the expected peak height is between 0.05 % and 0.63 % depending on channel dimensions and bead size. Assuming that the noise level scales linear with the measured impedance, the peak heights of the 3 µm beads will almost be in the noise band for channels with a height of 20 µm and a electrode area of 20 µm × 100 µm. For smaller channels, the signal to noise ratio should be better, because the volume ratio between the bead and the sample volume is larger. The drift and noise in the capacitance output of the AH2700A was about 5 fF noise and about 2 fF drift. The capacitance is of less interest, because the capacitance is dominated by the electrical double layer, which does not change when a bead passes.

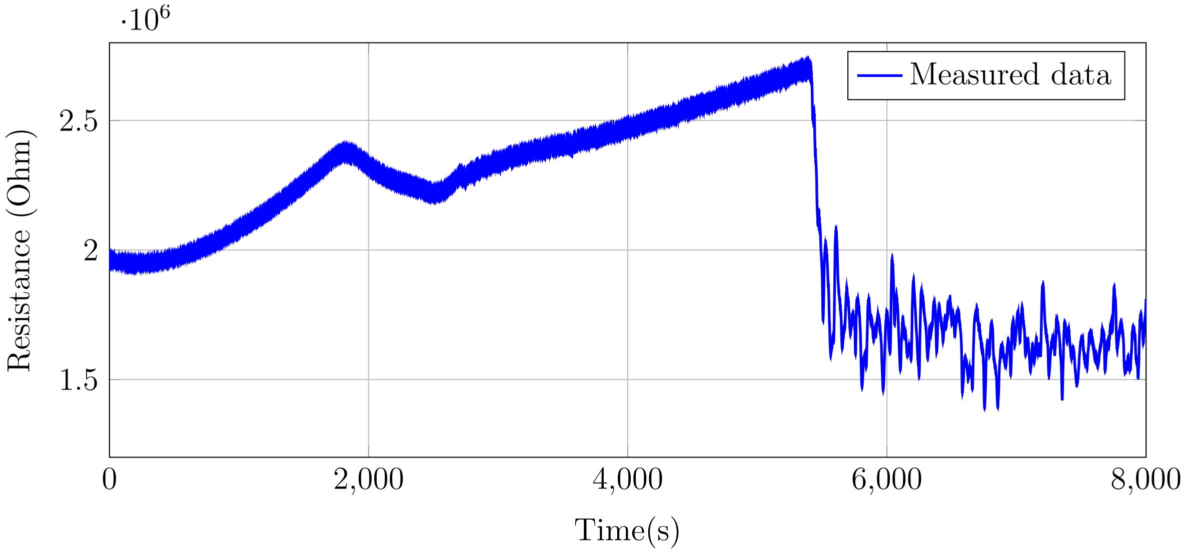

Figure 4.2: Long term drift in the real part of the impedance. MQ electrolyte was used in a channel with a height of 20 µm and an electrode area of 20 µm × 20 µm. Measurement was performed at 20 kHz with an amplitude of 0.25 V. The flowrate was changed every 45 min in the following steps: 0.05, 0.01 and 0.002 µl/min.

Figure 4.2 shows the resistance of the MQ electrolyte under different flow conditions. From 0 to 2700 seconds, the flow was set to 0.05 µl/min. The signal drifted 400 kΩ and then changed slope. At 2700 seconds, the flow was set to 0.01 µl/min. The drift was constant for this flow condition. The last flow condition of 0.002 µl/min was set at 5400 seconds. The measured resistance of the MQ electrolyte fluctuated heavily compared to the other flow conditions, but the average drift seems much less compared to the other flow conditions. Other measurements where the amplitude of the applied potential was varied, showed similar behaviour. Experiments with flow conditions set to 0.05 µl/min or 0.01 µl/min showed a constant positive or negative drift, whereas experiments with the flow set to 0.002 µl/min always showed fluctuations in the impedance measurement.

These results show that there is a correlation between the impedance and the flow. A clear explanation for this phenomena was not found, although it is expected that the fluctuations in the impedance for the lowest flow rate are caused by a non steady flow. These measurement were performed in MQ. In a low conductive environment, the double layer extends further into the channel and effects of changing flow rate were expected to be larger. Therefore, the result are not representable for a system using PBS to suspend the beads. Experiments were repeated in PBS to see if the same effects can be observed.

Figure 4.3 shows the results for a experiment with PBS. A drift was still observed in the impedance signal, but much smaller compared to the drift recorded using MQ. In MQ, the drift could be as much as a signal increase or decrease of 20 % over a time period of 45 minutes. In PBS, the drift can still be about 6 %, which is large compared to the impedance change caused by a bead passing event. Therefore it is required to remove the drift from the signal. A drift compensated signal can be obtained by passing the raw impedance data through a moving average filter and subtracting the output from the impedance, hereby removing the drift from the signal (Fig. 4.4). The drift compensated signal shows the fluctuations for the lowest flow rate condition. The moving average filter could not follow the fast fluctuations, as a result they

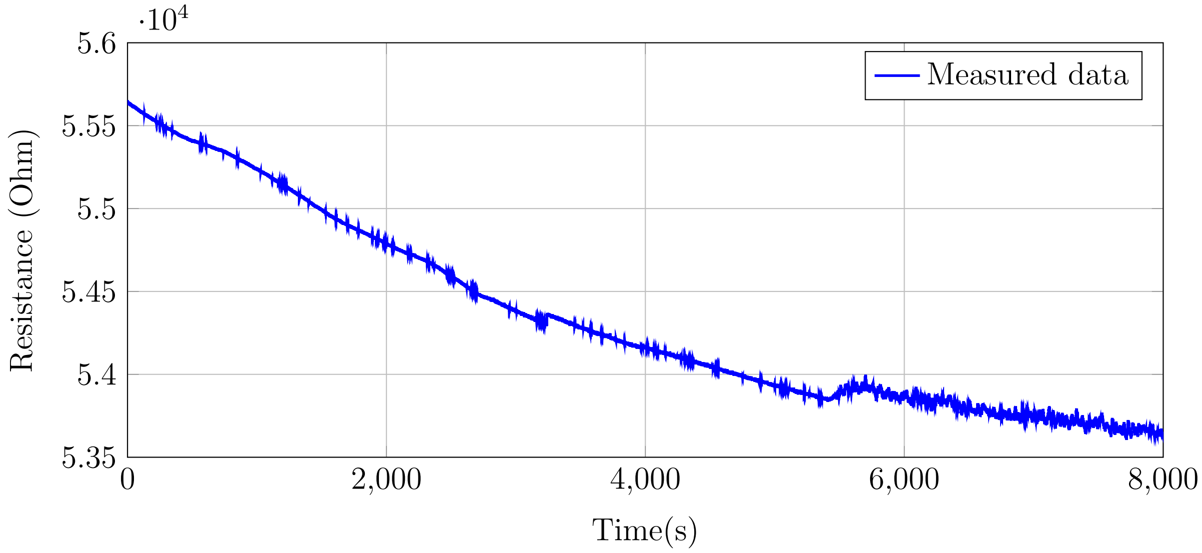

Figure 4.3: Long term drift in the real part of the impedance. PBS electrolyte was used in a channel with a height of 20 µm and an electrode area of 20 µm × 20 µm. Measurement was performed at 20 kHz with an amplitude of 0.25 V. The flowrate was changed every 45 min in the following steps: 0.05, 0.01 and 0.002 µl/min.

showed up in the drift compensated signal. There is a possibility to make the averaging time smaller, but at a certain point the average will also follow the fast peaks of the beads. This will result in peaks being removed from the signal. The fluctuations in the impedance can best be avoided by using a flow above 0.002 µl/min. The recorded noise bands for flow conditions of 0.01 µl/min and 0.05 µl/min were equal to the noise bands recorded with the resistor and capacitor setup. The limiting factor is probably the accuracy of the Andeen-Hagerling AH2700A device.

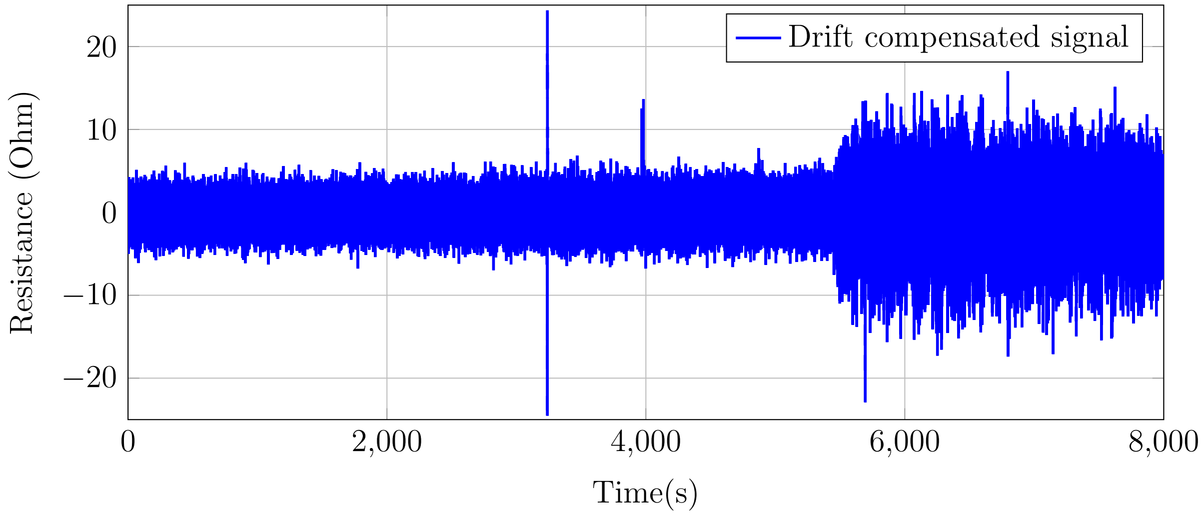

Figure 4.4: Drift removed from the real part of the impedance. Raw impedance signal is shown in fig. 4.3.

4.1.2 Peak height distribution

In this section, the focus will be on the peaks produced by the bead passing the impedance electrodes, especially the peak height and the variation there in.

Low frequency measurements

These measurements were performed with the AH2700A using its maximum measurement frequency of 20 kHz. The real part of the impedance(closely related to the resistance of the electrolyte) is shown in figure 4.5. The drift compensated signal with the peaks is shown in figure 4.6. When comparing figure 4.5 with 4.6, it can be seen that the drift compensation is necessary, because the peaks of the beads were much smaller then the fluctuations in the real part of the impedance. Figure 4.6 also shows that the moving average is not ideal. The peaks in the raw peak signal also contributed to the average, resulting in a slight increase in the average around the peak. When subtracting this average, the drift compensated signal went below zero around the peaks. This had an impact on the obtained peak height.

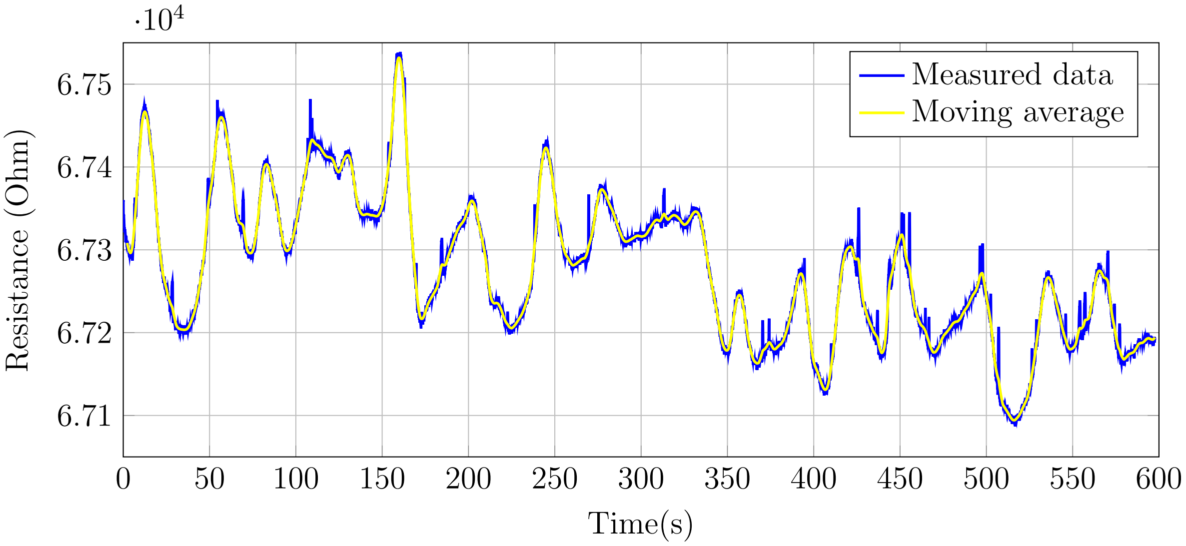

Figure 4.5: 3 µm beads suspended in PBS measured with the AH2700A at measurement frequency of 20 kHz. The flow was set to 0.002 µl/min. Chip dimensions were as follows, a channel height of 20 µm and an electrode area of 20 µm × 20 µm. 41 beads were detected during a period of 10 minutes.

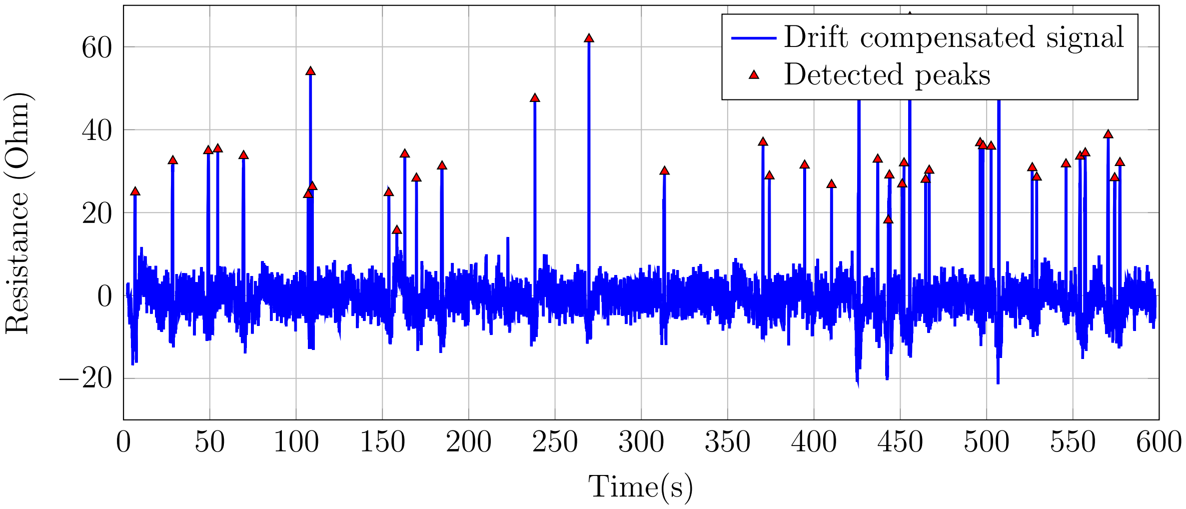

Figure 4.6: Drift compensated signal. Raw impedance signal is shown in fig. 4.5.

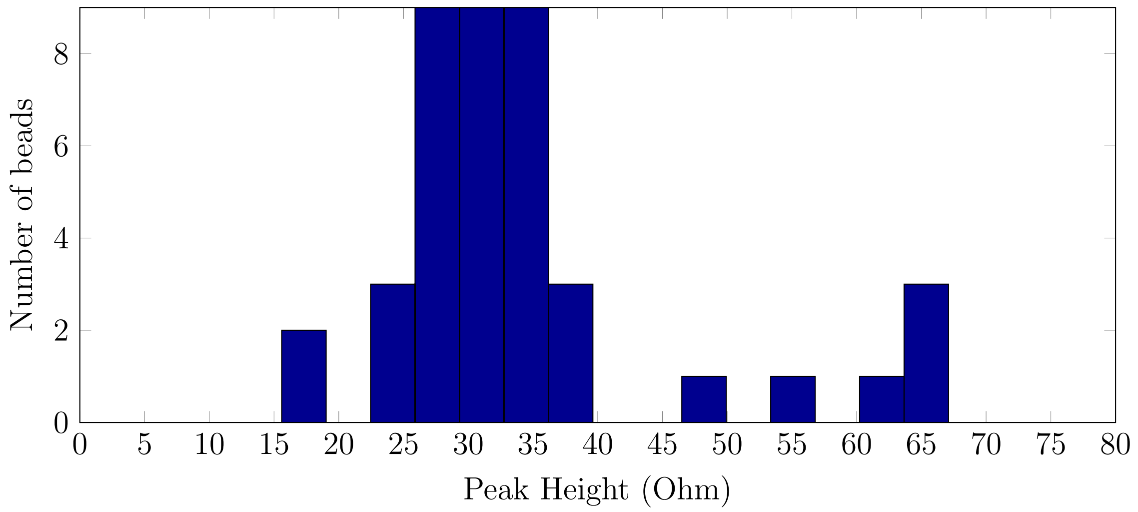

Figure 4.7: Peak height distribution of 3 µm beads suspended in PBS measured with the AH2700A at measurement frequency of 20 kHz. The flow was set to 0.002 µl/min. Chip dimensions were as follows, a channel height of 20 µm and an electrode area of 20 µm × 20 µm. 41 beads were detected during a period of 10 minutes.

Figure 4.7 shows how the detections are distributed over their peak heights. The average peak height was a little above 30 Ω. Two beads entering the sample volume simultaneous produced some detection around double the average peak height. The peak height predicted by the equivalent circuit model is 92.2 Ω when matching the channel and bead dimensions of the experiment to the simulation. This value is a factor 3 higher compared to the peak measured. This can be explained by an assumption used to make the model that is not valid. A good candidate for this would be the assumption that the electrolyte is a homogeneous material. This is not the case, since an electrical double layer will form around the bead. The conductivity of the bead is therefore not only determined by the bulk conductivity, but also by the movement of charge in the electrical double layer on the surface of the bead[10]. The surface conductivity would dominate over the bulk conductivity, which is very low for polystyrene beads. The resulting higher bead conductivity would lead to a lower predicted peak height. An other aspect that would explain the lower observed peak height is that the sample volume is actually larger than the volume between the electrodes. This could be the case because the electric field is never perfectly uniform.

The model only predicts a variance in the peak height, when the beads are not similar in size. The beads used in the experiments have a certain size variance. Besides size difference, other factors can play a role in the variance of the peak height. The model assumes a homogeneous electric field between the impedance electrodes, in practice the electric field will not be homogeneous. This results in a peak height which is depended on the position of the bead. Furthermore, the temperature influences the conductivity of the electrolyte. The peak height is dependent on the conductivity of the electrolyte and therefore peak height will change.

Influence of speed

In this subsection, the influence of the speed of a bead on the peak height it produces is investigated. Measurements were performed using a Zurich Instruments HF2IS at a measurement frequency of 1 MHz. For bead detection, rather than the real part of the impedance, the absolute impedance signal was used. At 1 MHz these are almost the same, as the phase of the impedance is small in the resistive plateau. Figure 4.8 shows the distribution of detected beads as a function of peak height. Again, the average peak height is around 30 Ω. Video data was used to obtain speed data of the beads. The results are shown in figure 4.9.

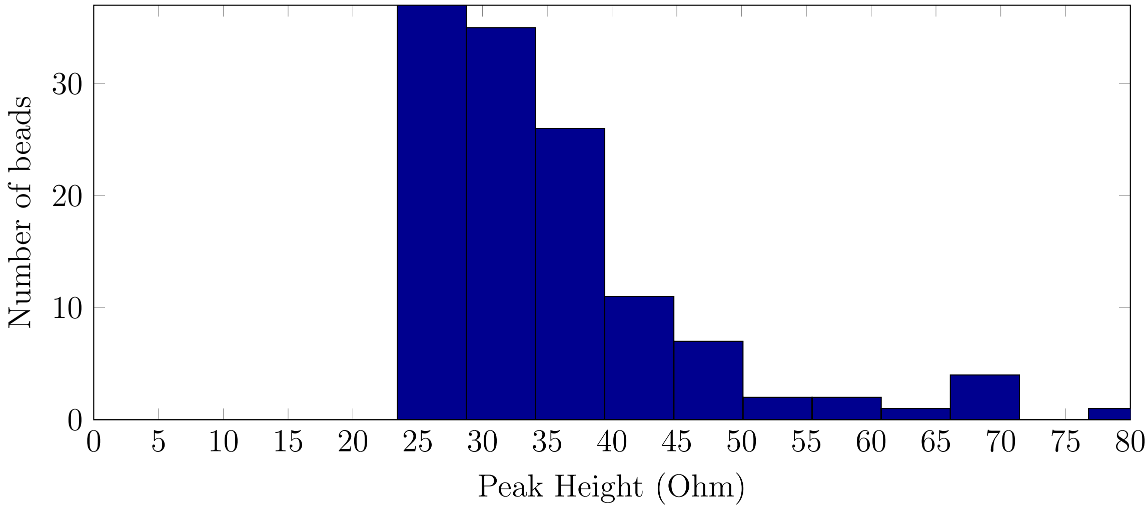

Figure 4.8: Peak height distribution of 3 µm beads suspended in PBS measured with the HF2IS at measurement frequency of 1 MHz. Bandwidth of the low pass filter in the HF2IS was set to 20 Hz. The flow was set to 0.01 µl/min. Chip dimensions were as follows, a channel height of 20 µm and an electrode area of 20 µm × 20 µm. 128 beads were detected during a period of 7 minutes.

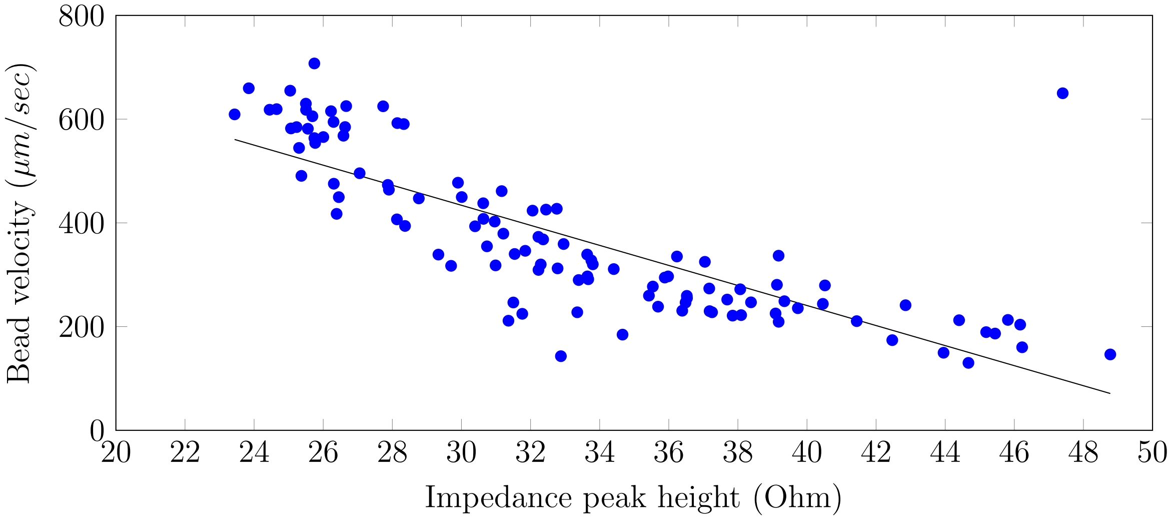

Figure 4.9: Peak height vs bead velocity, bandwidth of the measurement was 20 Hz.

There is a clear relation ship between the speed of the bead and the corresponding peak height (Fig. 4.9). The linear trend line through the points shows that fast beads produced a lower peak height. This is caused by a low bandwidth(20Hz) of the low-pass filter in the HF2IS. At a speed of 800 µm/s and a electrode length of 20 µm, the beads remained between the electrodes for 25 ms. A signal with a period of 25 ms has a frequency of 40 Hz. Therefore the amplitude of the signal is attenuated by the low-pass filter. So a trade-off between noise and filter setting/flow has to be made. Figure 4.10 shows that there is no correlation between the peak height and speed if the bandwidth of the low pass filter in the Zurich is set to 200 Hz.

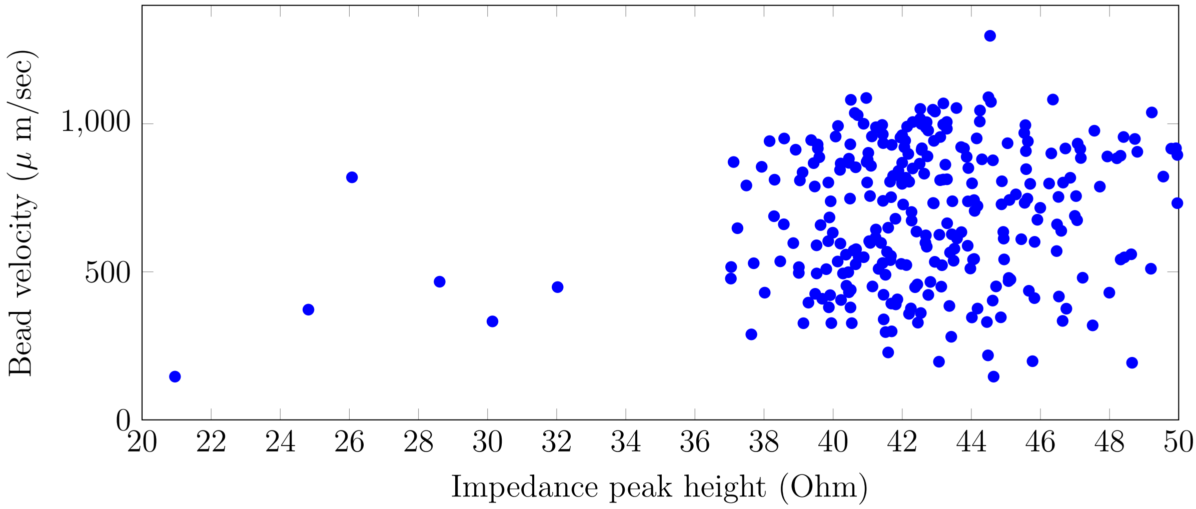

Figure 4.10: Peak height vs bead velocity, bandwidth of the measurement was 200 Hz.

Influence of position

In this subsection, the influence of the position of a bead on the peak height is investigated. Since the microscope only made a video of the top view of the chip, only the x-position(width direction of the channel) can be determined. The height at which the beads passed the electrodes remains unknown. From the x-position data no relation between impedance peak height and position could be found (Fig. 4.11).

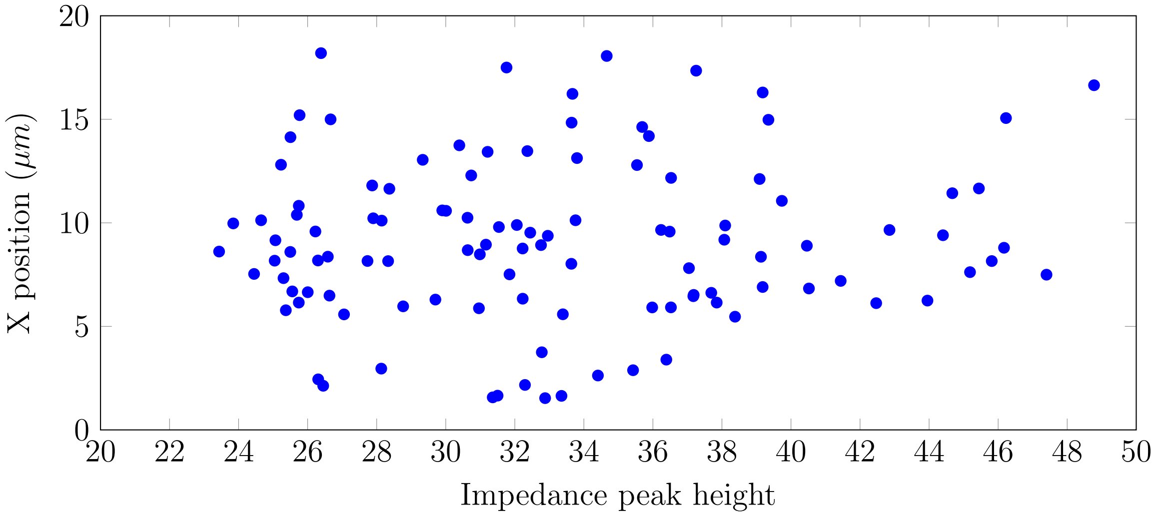

Figure 4.11: Peak height vs bead position.

Effect of focusing

The position data obtained from the video did not result in a relation between position and peak height. So in this experiment the beads were focused in a more uniform position in the channel with the help of dielectrophoresis. Due to a faulty connection to one of the DEP focusing electrode the beads were focused to the side of the channel in stead of middle. The variance in peak height is checked for two situations: the focusing is turned off (Fig. 4.12) or the focusing is turned on (Fig. 4.13). When comparing these results, a clear improvement in variance of the peak height can be observed when the beads are focussed. Similar results were observed by [11]. The improvement in variance is most likely caused by the beads passing through the same part of the non uniform electric field. The mean value of the peak height is a bit lower for the focused beads compared to the unfocused beads. This is probably due to focusing to a unnatural position.

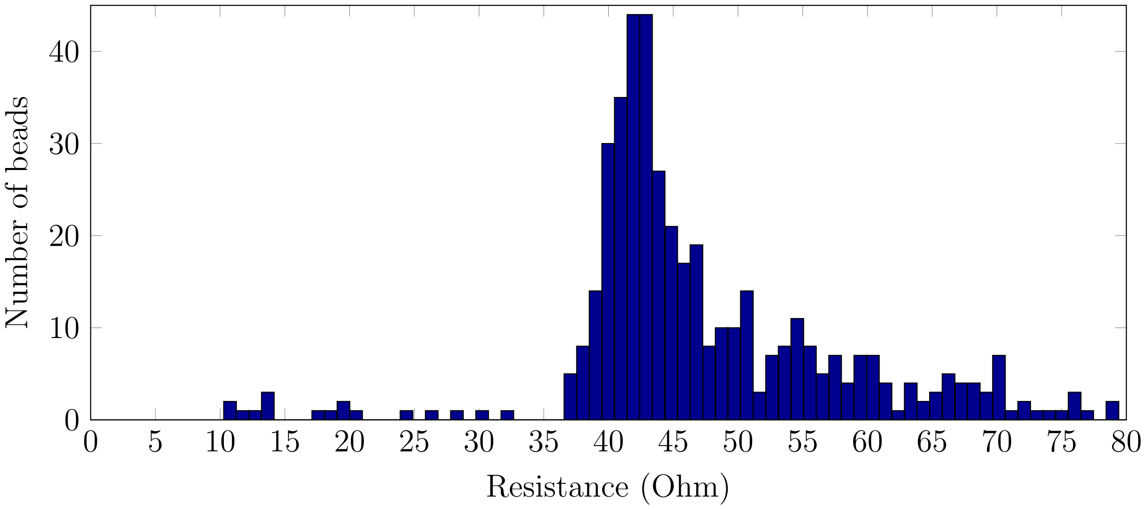

Figure 4.12: Peak height distribution of 3 µm beads suspended in PBS measured with the HF2IS at measurement frequency of 1 MHz. Bandwidth of the low pass filter in the HF2IS was set to 200 Hz. The flow was set to 0.01 µl/min. Chip dimensions were as follows, a channel height of 20 µm and an electrode area of 20 µm × 20 µm. 439 beads were detected. The DEP focusing was turned off.

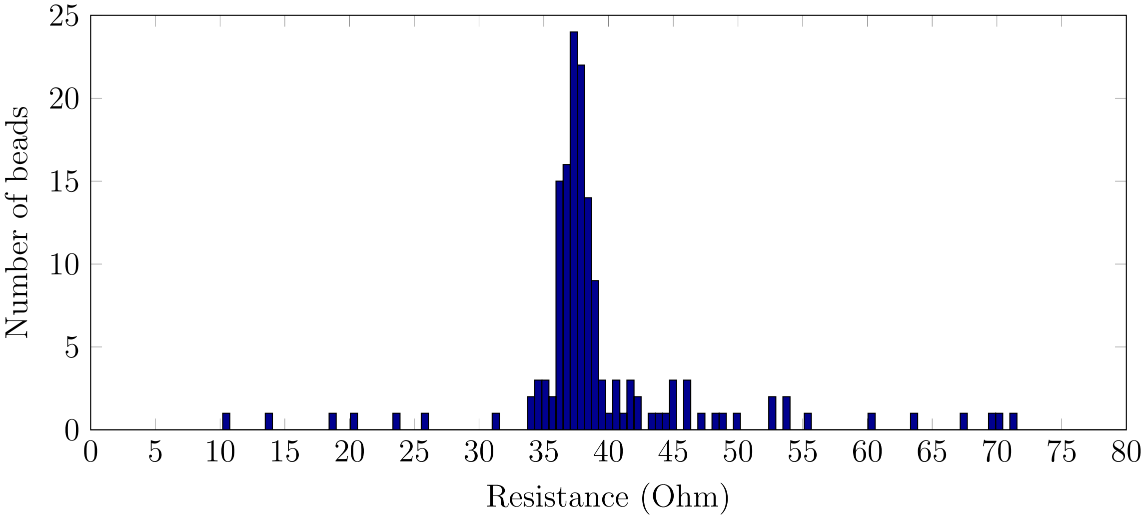

Figure 4.13: Peak height distribution of 3 µm beads suspended in PBS measured with the HF2IS at measurement frequency of 1 MHz. Bandwidth of the low pass filter in the HF2IS was set to 200 Hz. The flow was set to 0.01 µl/min. Chip dimensions were as follows, a channel height of 20 µm and an electrode area of 20 µm × 20 µm. 153 beads were detected. The DEP focusing was turned on.

Separation between 3 µm and 4 µm beads

In order to separate 3 µm and 4 µm beads based on impedance data, a clear distinction must be made between the impedance response of both species. In figure 4.14 the number of beads detected is shown as a function of peak height. Results were obtained by focusing the beads prior to the impedance detection. A clear distinction between 3 µm and 4 µm beads is visible. The mean peak height for 3 µm is around 6.5 Ω and for the 4 µm beads around 21 Ω. These results show a clear differentiation between 3 µm and 4 µm bead based on impedance peak heights. The distributions for the 3 µm and 4 µm are so far apart that detection of smaller size differences should be possible in the future.

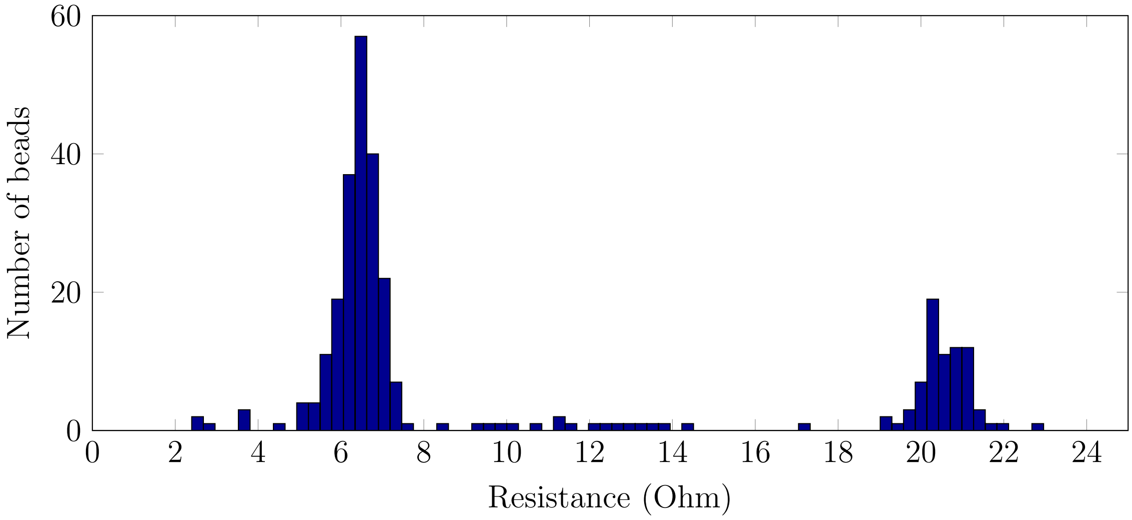

Figure 4.14: Peak height distribution of 3 µm and 4 µm beads suspended in PBS measured with the HF2IS at measurement frequency of 1 MHz. Bandwidth of the low pass filter in the HF2IS was set to 200 Hz. The flow was set to 0.01 µl/min. Chip dimensions were as follows, a channel height of 20 µm and an electrode area of 50 µm × 20 µm. 300 beads were detected. The DEP focusing was turned on.

4.2 Dielectrophoresis

Dielectrophoresis has to fulfil two tasks in the proposed system: focusing of the beads before impedance detection and separation afterwards by pushing the beads into a different flow lamina. The results shown in this subsection were all obtained using a chip with a channel cross-section of 20x100 µm. Position data of the beads was obtained using the video data.

4.2.1 Focusing

Four electrodes are used to generated the electric field for the DEP focusing. Electrodes diagonally opposite of each other get the same potential. Using this orientation the center of the channel has the lowest electric field. The electrodes are shaped in such a way that they get closer to each other as the channel progresses (black lines in fig. 4.15). The coloured lines in figure 4.15 show the tracks the beads followed. At all tested voltages(1 V, 2.5 V and 5 V) the beads were focused in the center of the channel. At higher voltages the balance between the Stokes drag force and the DEP force was reached further away from the electrode edge, resulting in a more compact focusing(Fig. 4.16).

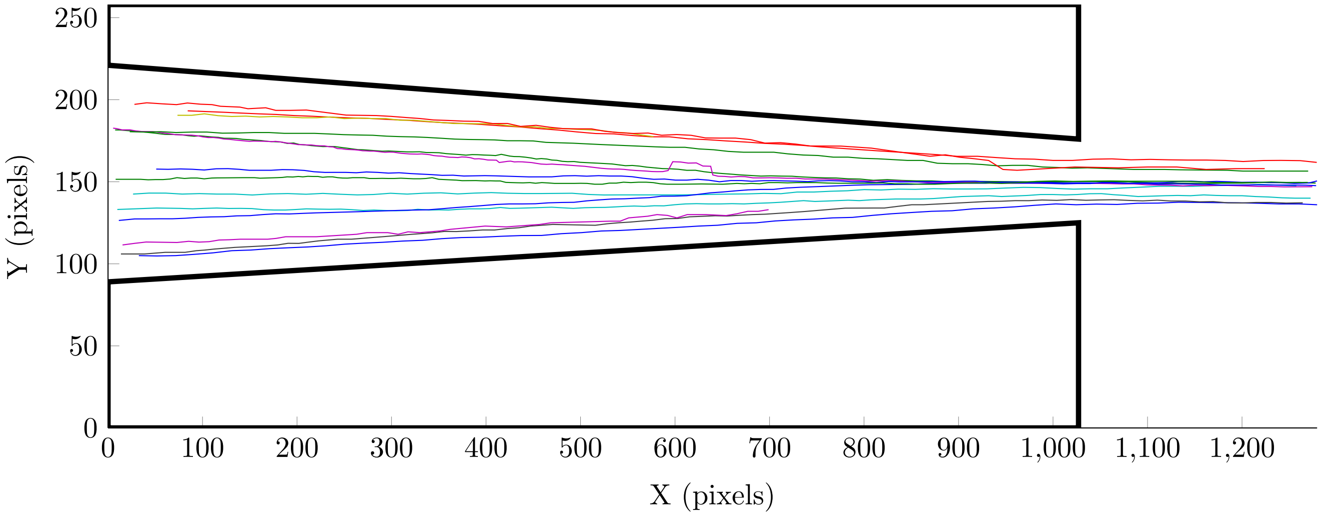

Figure 4.15: Dep focusing of beads with the flow set to 0.01 µl/min with a DEP potential of 10 MHz 2.5 V.

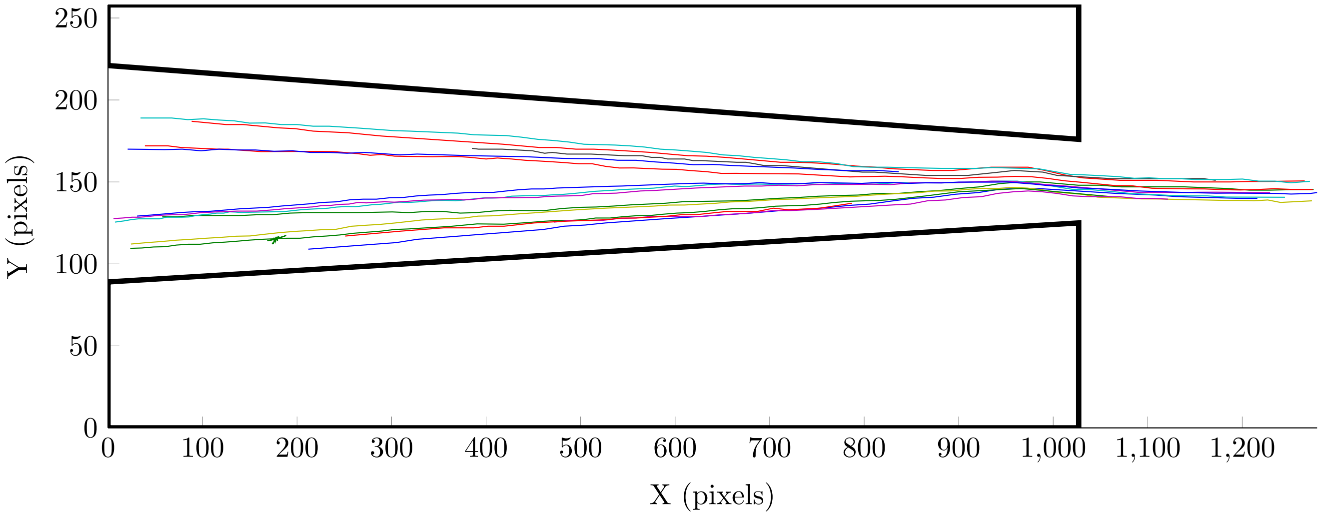

Figure 4.16: Dep focusing of beads with the flow set to 0.01 µl/min with a DEP potential of 10 MHz 5 V.

4.2.2 Sorting

The sorting electrodes are placed under an angle of 15° with the channel wall. Due to a high electric field gradient at the edge of the electrode, the beads were pushed away from the electrodes by a n-DEP force. As a result they moved along the edge of the electrode. The results were obtained on a chip where the beads where focused first and then sorted (pushed into another flow lamina). At all tested voltages (1 V, 2.5 V and 5 V) the beads were pushed to the side of the channel. The results for the experiment with a DEP potential of 1 V shows that the beads were very close to the electrode edge (Fig. 4.17). A slight increase in flow would probably push the beads over the position were the electric field gradient is maximum and let the stokes drag force push the beads in a straight line. Tracks shown below y pixel 50 are probably of particles with different dielectric properties as the beads, as they are not focused or sorted. For higher DEP potentials, the beads were pushed farther away from the electrode edge (Fig. 4.18). The same behaviour was observed for DEP focusing.

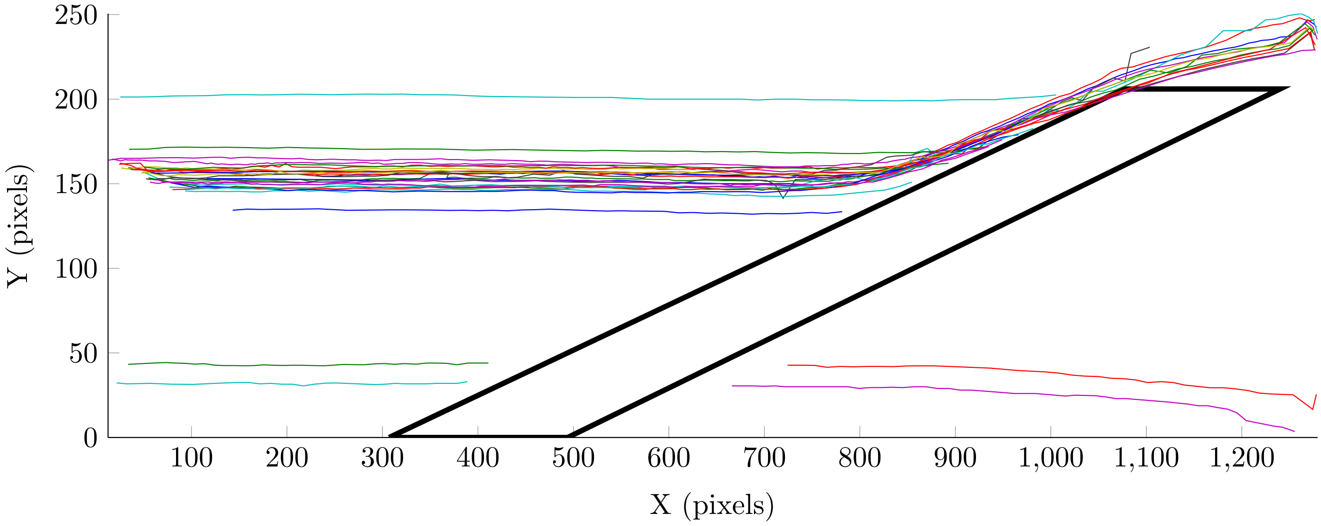

Figure 4.17: Dep sorting of beads with the flow set to 0.01 µl/min with a DEP potential of 10 MHz 1 V.

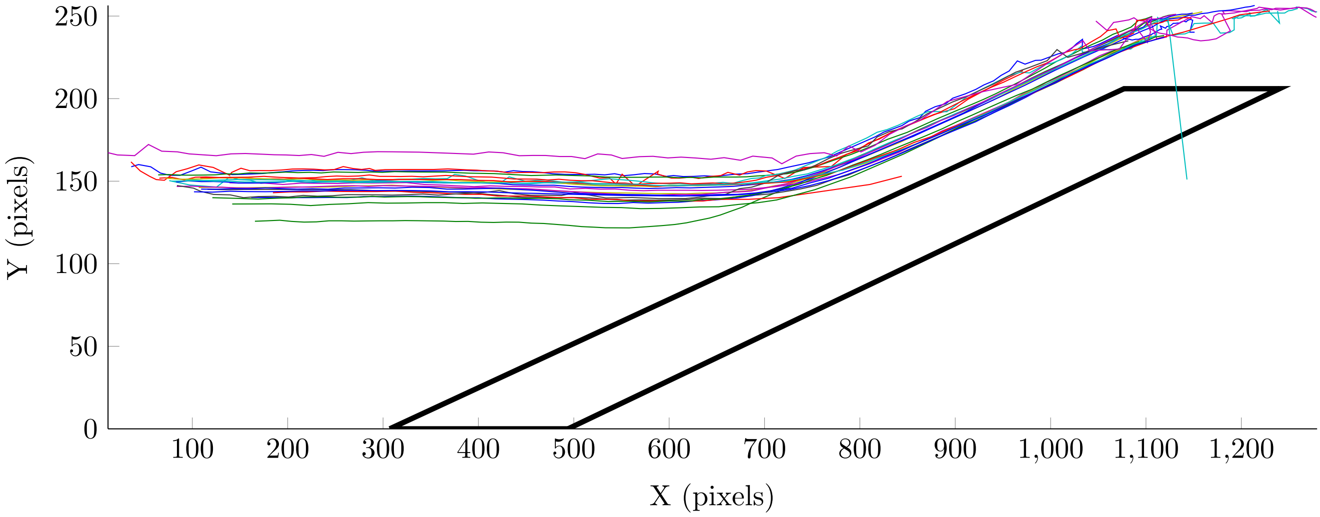

Figure 4.18: Dep sorting of beads with the flow set to 0.01 µl/min with a DEP potential of 10 MHz 5 V.

4.3 Total system

Results obtained from impedance and dielectrophoresis experiments showed the potential to make a system that is able to sort 3 µm and 4 µm beads based on their size. Therefore these two part need to be linked. In order to do so, the time when the sorting needs to be activated should to be known. The time it takes to travel from detection part of the chip to the separation part of the chip needs to be calculated. With this information the sorting electrode can be turned on at the correct time.

4.3.1 Speed measurement

To calculate the travel time of a bead between the detection and the separation part of the chip, the speed of the individual bead needs to be known. Besides the peak height, a peak in the impedance signal also has a peak width. The peak height is used to determine the size of the passing bead. The peak width can be used to determine the speed of the passing bead. A comparison is made between the speed obtained from impedance data and the speed obtained from the video data. Equation 4.1 and 4.2 are used to obtain the speed of the bead in µm/s. Unfortunately, it is hard to obtain accurate values for some of the factors in these equations. For the speed obtained from the video, the factor $\frac{\text{distance}(\mu\text{m})}{\text{pixel}}$ is hard to obtain accurately. The only well known dimension in the video frame is often the electrode. The electrode is 20 µm in width which is spread over tens of pixels, the low pixel count per µm can give inaccurate results. Obtaining the speed data from the impedance is also very challenging due to the impedance peak shape. This shape is like a bell, no clear edges defining the start and end of the peak. The electrode length was varied from the actual dimension to obtain a slope of 1, hereby calibrating the speed measurement. The results of the measurement are shown in figure 4.19.

$$V_{\text{bead video}}(\mu\text{m/s}) = \frac{\text{pixels}}{\text{frame}} \cdot \frac{\text{distance}(\mu\text{m})}{\text{pixel}} \cdot \text{frame rate(frames/s)} \tag{4.1}$$

$$V_{\text{bead impedance}}(\mu\text{m/s}) = \frac{\text{electrode lenght}(\mu\text{m})}{\text{peak width(s)}} \tag{4.2}$$

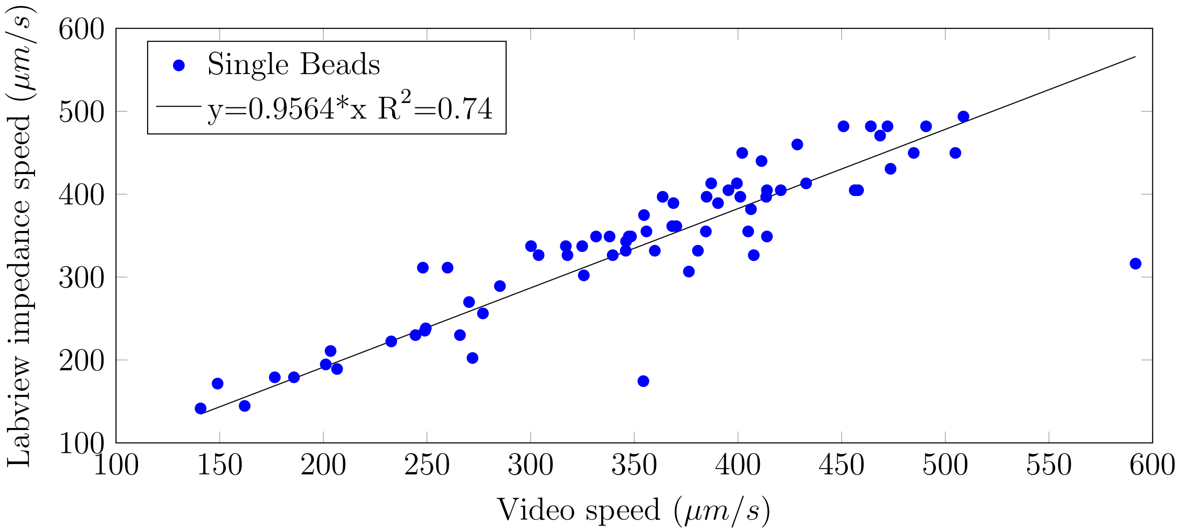

Figure 4.19: Speed data obtained from of impedance data vs speed data obtained from video data.

By varying the electrode length, used in the calculations, from the actual dimension, the slope of the trend line is almost one. After such a calibration the peak width can be is a good measure for the speed of a bead. But there is still some inaccuracy in the speed measurement. This can also be seen in the low value for the R^2 of the fit. The inaccuracy becomes more prominent for a measurement where the beads are focused, because the beads have a more uniform speed (Fig. 4.20). This inaccuracy will also cause an error in the calculated travel time. This can be compensated by turning the sorting electrode on for a longer time. Unfortunately, this limits the throughput of the system.

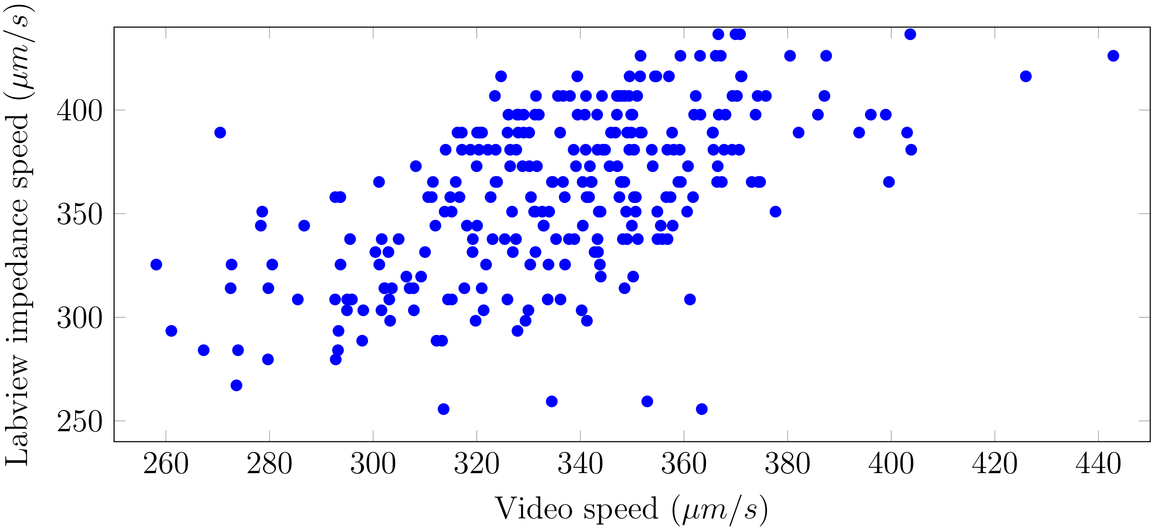

Figure 4.20: Accuracy of bead speed measurement after focusing both 3 µm and 4 µm beads are included.

4.3.2 Sorting

In this final section of the chapter, results are shown for experiments where all parts of the proposed system are active during the experiment. When beads enter the chip, they were focused by the DEP focusing electrodes prior to impedance detection. Peaks in the impedance data were used to make a decision if the bead should be sorted based on the peak height. The width of the peak was used to determine when the bead would reach the separation electrodes. The separation electrodes were turned on if the passing bead should be sorted.

Figure 4.21 shows the measured impedance and the position(in the width direction of the channel) of the bead. The impedance is plotted on the left y-axis in red, whereas the position data is plotted o the right y-axis. Each bead has its own color for the position data. The system was programmed to separate the 3 µm beads. The thresholds for the peak height of detected beads, which must be sorted was set between 5 Ω and 8 Ω. In figure 4.21, at approximately 4 seconds a 3 µm bead was detected. After a second, the sorting electrode was turned on. It can be clearly observed that the impedance signal is influenced by the activated sorting electrodes. Soon after the sorting electrode is activated, the bead came into the view of the camera in the middle of the channel(~50pixels). At approximately 6 seconds the bead reached the sorting electrode and was deflected from the middle(~50pixels) of the channel to the side(~20pixels). At approximately 16 second a 4 µm bead was detected. A second later it came into view of the camera. The sorting electrode is not turned on, so the 4 µm bead can pass in a straight line.

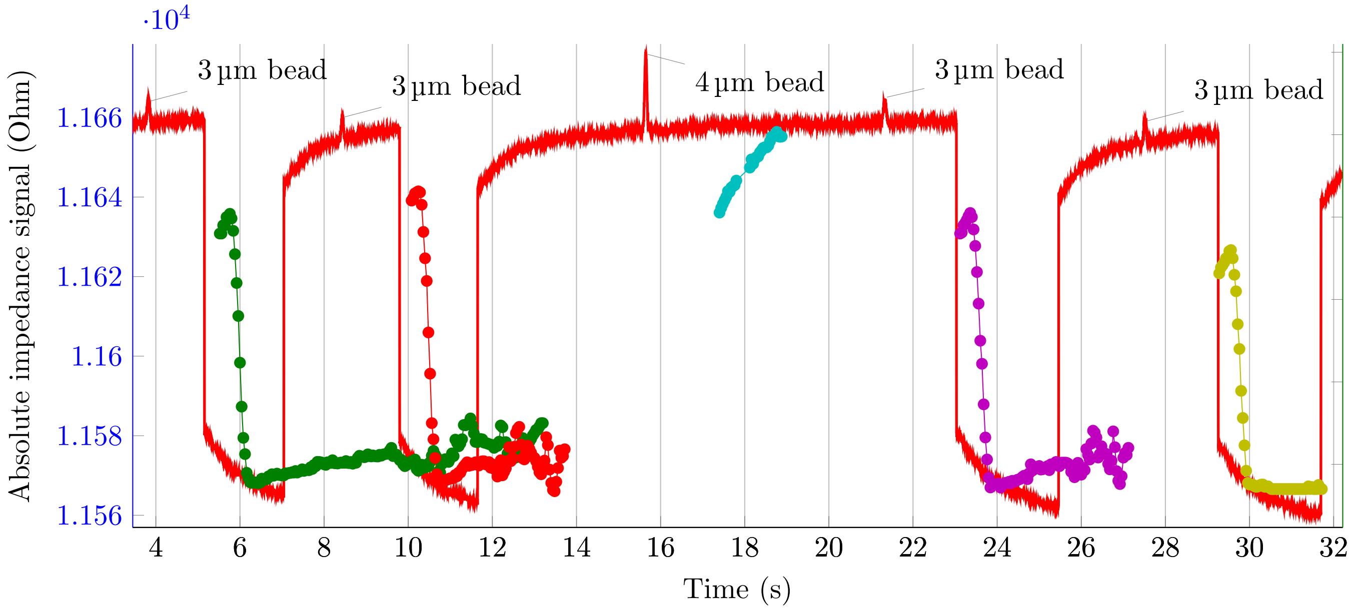

Figure 4.21: Impedance signal and bead position in channel. With the following measurement conditions: 3 µm and 4 µm beads suspended in PBS, measured with the HF2IS at measurement frequency of 1 MHz. Bandwidth of the low pass filter in the HF2IS was set to 200 Hz. The flow was set to 0.01 µl/min. Chip dimensions were as follows, a channel height of 20 µm and an electrode area of 50 µm × 20 µm. The DEP focusing was turned on.

An analysis was done to find the cause of the crosstalk between the impedance measurement and the sorting electrode turning on and off. By grounding an electrode between the impedance measurement and the sorting electrodes, the step in impedance when switching disappeared. Unfortunately, turning on the sorting electrode also caused a drift in the impedance signal. Flow conditions were changed to see if this observation was caused by a thermal effect. However this was not the case. Furthermore, electrical crosstalk was investigated using a battery operated oscillator to supply the sorting electrodes, but still the drift was visible in the impedance signal. The cause of this effect was not found. The first peak detector mentioned in the materials and methods chapter using a high pass filter could not handle this drift because it was detected as a peak. This detected peak caused sorting electrode to be turned on making the system oscillate. The second peak detector mentioned in the materials and methods chapter using pattern fitting was not disturbed by the drift in the impedance signal and made the total system work.

Figure 4.22 shows the 3 µm and 4 µm beads entered the separation area as one group and exiting in two groups. The 4 µm beads in the center of the channel and the 3 µm beads at the side of the channel. Unfortunately, no success was obtained trying to guide the two separate groups to individual outlets of the chip. The SU-8 in the small outlet channel was not develop away nicely, this resulted in problems with the flow balancing at the channel split.

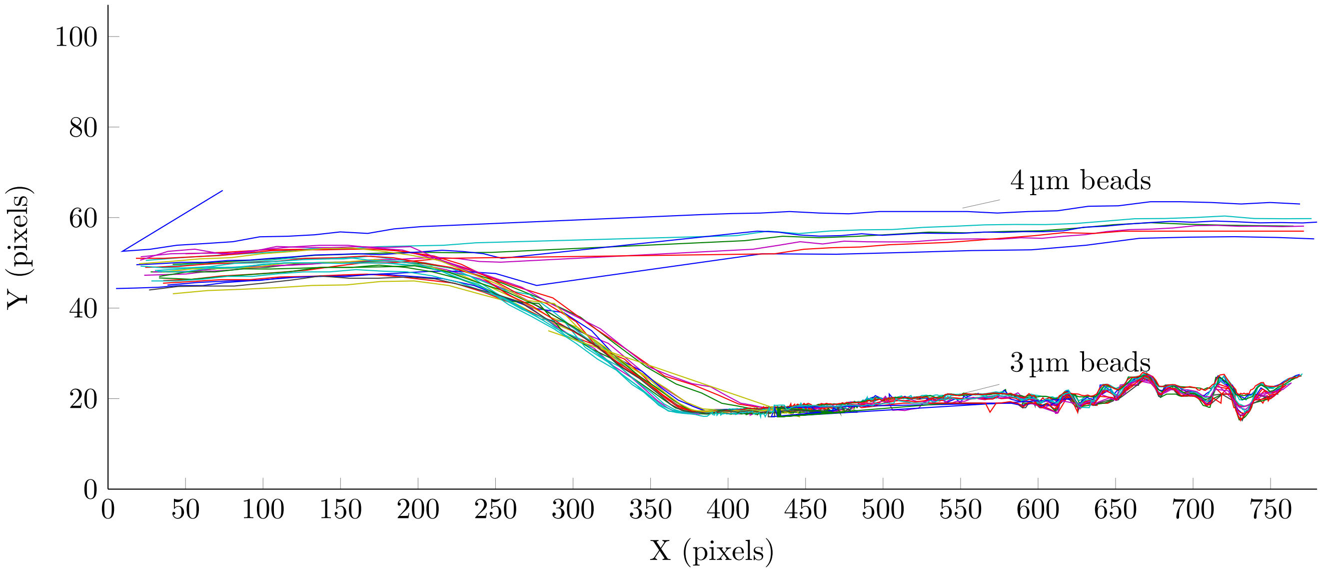

Figure 4.22: 3 µm and 4 µm beads separated in two groups.

Chapter 5

Conclusion and Recommendations

5.1 Conclusion

In the introduction the following goal was formulated: ”Creating and characterizing a microfluidic system that is able to sort polystyrene beads based on their size”. To achieve this goal, a microfluidic chip was used which is developed in the BIOS group. The tasks the system should perform were divided into four blocks: differentiation, transport, separation and control. The individual blocks of the system were characterized before combining them into a complete system.

The differentiation between 3 µm and 4 µm beads was successful. The impedance measurements in the microfluidic chip resulted in peaks with an average of 6.5 Ω for the 3 µm beads and an average of 21 Ω for the 4 µm beads. DEP focusing prior to the impedance measurement reduced the variance in peak height, allowing detection of smaller differences in the future. The bandwidth of the impedance measurement, was shown to be very important in this system: a too low cut-off frequency reduces the peak height of fast moving beads. Furthermore, information about the speed of the beads was extracted from the impedance signal.

The sorting of the beads could be done by dielectrophoresis. It was shown that the trajectory of the beads in the channel could be changed. The DEP focusing directed the beads to the center of the channel, while the DEP sorting pushed the beads to the side of the channel.

The Labview control system detected the peaks in the impedance signal to determine the size and speed of the passing beads. The size information was used to determine whether the bead should be sorted and the speed was used to determine when the sorting should be activated. Using this information, the total system was able to separate 3 µm and 4 µm beads in different flow lamina. Unfortunately, due to the limitations of the microfluidic device, the beads ended up in the same outlet after separation.

5.2 Recommendations

The first point to address is the problem with the system where the beads are place in different flow lamina but still end up in the same outlet. The chip was designed in such a way that a third of the flow would end up in one outlet and two thirds in the other outlet. The beads in the center should end up in the first outlet and deflected beads in the other. The fluidic resistance of the connecting capillary seems to play a large role in the flow distribution between the two channels. The resistance of the outlet channels could be increased to provide a more stable flow distribution between both outlets.

The performance of the system could be improved by a more accurate measurement of the speed of the beads. Due to this inaccuracy of the speed measurement, the sorting electrode has to be actuated for a long period to make sure that a bead is sorted. Reducing this duration allows for higher bead concentrations increasing throughput of the system. A more accurate speed measurement of the bead should be possible with a differential impedance measurement. With a differential measurement the impedance is measured with two sets of electrodes. These signals are then subtracted from each other. A bead will produce two peaks, one for each set of electrodes. The time between the peaks and the distance between the electrodes can be used to calculate the speed. A disadvantage is that this method also limits the maximum concentration, as the sample volume is increased. An advantage is that it is likely to reduce the drift in the signal. Another solution would be to give the beads all the same speed so that a measurement of the speed is not necessary any more. A more uniform position in the channel will probably also improve the variance in the peak height even more.

Bibliography

[1] G. Seidel and D. Garner, "Current status of sexing mammalian spermatozoa," *Reproduction*, vol. 124, no. 6, pp. 733–743, 2002.

[2] T. Sun, C. Bernabini, and H. Morgan, "Single-colloidal particle impedance spectroscopy: Complete equivalent circuit analysis of polyelectrolyte microcapsules," *Langmuir*, vol. 26, no. 6, pp. 3821–3828, 2010.

[3] R. Pethig, "Review article–dielectrophoresis: Status of the theory, technology, and applications," *Biomicrofluidics*, vol. 4, no. 2, 2010.

[4] A. J. Bard and L. R. Faulkner, *Electrochemical Methods: Fundamentals and Applications.* Wiley, 2 ed., 12 2000.

[5] T. B. Jones, *Electromechanics of Particles.* Cambridge University Press, 9 2005.

[6] H. Bruus, *Theoretical Microfluidics (Oxford Master Series in Condensed Matter Physics).* Oxford University Press, 11 2008.

[7] J. Clements and J. Bekkers, "Detection of spontaneous synaptic events with an optimally scaled template," *Biophysical Journal*, vol. 73, no. 1, pp. 220 – 229, 1997.

[8] Mathworks, *Help file Mathlab: Computer vision tool box-Motion-Based multiple Object Tracking.* Mathworks, 2013b ed., 2013.

[9] J. Wei, "Using hf2is impedance spectroscope for fra, 2-terminal and 4-terminal measurements." http://www.zhinst.com/blogs/jamesw/hf2is-fra/, 9 2013.

[10] I. Ermolina and H. Morgan, "The electrokinetic properties of latex particles: comparison of electrophoresis and dielectrophoresis," *Journal of Colloid and Interface Science*, vol. 285, no. 1, pp. 419 – 428, 2005.

[11] K. Cheung, S. Gawad, and P. Renaud, "Microfluidic impedance spectroscopy flow cytometer: particle size calibration," in *Micro Electro Mechanical Systems, 2004. 17th IEEE International Conference on. (MEMS)*, pp. 343–346, 2004.